TECHNICAL NOTES

NATIONAL ADVISORY COMMITTEE FOR AERONAUTICS

No. 900

EFFECT OF RIVET PITCH UPON THE FATIGUE STRENGTH OF SINGLE-ROW RIVETED JOINTS OF 0.025- TO 0.025-INCH 24S-T ALCLAD

By Victor Seliger
Lockheed Aircraft Corporation

Washington
July 1943

NATIONAL ADVISORY COMMITTEE FOR AERONAUTICS

TECHNICAL NOTE NO. 900

EFFECT OF RIVET PITCH UPON THE FATIGUE STRENGTH OF SINGLE-ROW RIVETED JOINTS OF 0.025- TO 0.025-INCH 24S-T ALCLAD

By Victor Seliger

SUMMARY

S-N curves at the range ratio of 0.2 were experimentally obtained for each of the following values of rivet pitch P as used in a single-row lap joint of 0.025- to 0.025-inch 24S-T alclad with one-eighth AN430 round-head rivets: P = 0.5, 0.75, 1.0, 1.5. Families of constant rivet pitch curves, which define the fatigue life for specimens studied, were developed. Curves showing the variation of the effective stress concentration factor in fatigue with rivet pitch and maximum load per rivet were also established.

INTRODUCTION

This investigation was conducted to determine the effect of rivet pitch upon the fatigue strength of single-row lap joints of 0.025- to 0.025-inch 24S-T alclad, using one-eighth AN430 round-head rivets. A further object was to determine the variation of the effective stress concentration factor in fatigue as a function of rivet pitch and of load per rivet.

SPECIMENS

Single-row lap-joint fatigue specimens were fabricated from 0.025-inch 24S-T alclad sheet, using AN430DD-4 rivets. The specimen dimensions and the rivet pitches are indicated in figure 4. The allowable design load for AN430DD-4 rivets in 0.025 24S-T alclad sheet is 256 pounds per rivet (ANC-5).

Because of a typographical error in ordering speci-

mens, the AN430 rivets were specified as the DD type instead of the AD type. Failure always occurred in the sheet, however, and check tests made with two specimens using AD-type rivets agreed closely with results for specimens using DD-type rivets.

APPARATUS AND TEST PROCEDURE

All fatigue specimens were tested at 1800 cycles per minute in the Lockheed vibrating beam machines, one of which is shown in figure 1. Tests were conducted at an R value of 0.2 (R, the range ratio, is the algebraic ratio of minimum to maximum load).

The dynamic load was measured by means of an electrical strain gage bridge, installed on the upper specimen mount as shown in figure 2. This bridge was statically calibrated before each test by means of dead weights applied at known distances from the beam pivot and the specimen center line. A percentage-of-modulation meter, used as a peak voltmeter, measured the bridge unbalance; and the bridge unbalance corresponding to the known static load was duplicated by the maximum and minimum peaks under dynamic loading.

All static tension tests were conducted in the 300,000-pound Southwark-Emery testing machine in the Triplett and Barton laboratory. Load-deformation and load-permanent-deformation curves were obtained, using two dial gage extensometers over a 3.2-inch gage length across the joint as shown in figure 3.

Average material properties are given in figure A-1.

RESULTS

The results of the static tension tests are tabulated below:

Specimen	Number of rivets per specimen	Rivet pitch (in.)	Static ultimate load per rivet (lb)	Average static ultimate load per rivet (lb)
1-A	12	0.5	390	
1-B	12	.5	378	382
1-C	12	.5	380	
2-A	7	.75	419	
2-B	7	.75	409	398
2-C	7	.75	367	
3-A	6	1.0	403	
3-B	6	1.0	380	392
3-C	6	1.0	392	
4-A	4	1.5	389	
4-B	4	1.5	405	400
4-C	4	1.5	405	

Load-deformation and load-permanent-deformation curves for each type of specimen are shown in figures 9 to 12.

The fatigue test results are plotted in the form of conventional S-N diagrams in figures 13 to 16. The curves, as drawn, define the lower limit of the test scatter. All fatigue failures occurred in one or both sheets with no cases of rivet shear recorded. Typical failures are shown in figures 5 to 8.

Figures 19 and 20 show families of constant rivet pitch curves with maximum load per rivet and maximum load per linear inch of joint, respectively, plotted against cycles to failure. These curves were obtained by plotting rivet pitch against the maximum load per rivet and against the maximum load per inch, respectively, for a constant number of cycles to failure, thus defining the curves given as figures 17 and 18, which afford a means of interpolating and extrapolating for values of rivet

pitch P other than those used in actual tests. In figures 21 and 22 the families of constant rivet pitch curves are replotted with the number of cycles to failure shown on a linear scale.

Figure 23 shows the variation of K_F, the effective stress concentration factor in fatigue, with rivet pitch for various constant fatigue lives. The effective stress concentration factor in fatigue is defined as

$$K_F = \frac{S_F}{S_N}$$

where S_F is the maximum value of the cyclically varying stress that the material itself can withstand for a given number of cycles as obtained from an axial tension fatigue curve for 24S-T alclad sheet at $R = 0.2$ (see appendix) and S_N is the maximum alternating stress that a joint can withstand for a given number of cycles based on its net area between rivet holes and obtained from the data herein presented.

Figure 24 shows the variation of the effective peak stress ($K_F S_N = S_F$) with nominal stress S_N for various values of rivet pitch, with the curves extrapolated to zero stress. Figure 25 is a cross plot of figure 24 showing the variation of the effective peak stress with rivet pitch for constant values of nominal stress.

Figure 26 is a family of constant rivet pitch curves showing the variation of K_F with the maximum load per rivet for the range ratio under investigation. The curves were extended to include the results obtained from static ultimate values and extrapolated to zero load through the use of figure 24.

Figure 27 shows the variation of K_F with the ratio of rivet diameter d to $P - d$ the net width of sheet supporting each rivet.

Figure 28 shows a comparison between the effective stress concentration factor curve for a stress approaching zero and the stress concentration factor curve determined photoelastically by Frocht and Hill for a close-fitting pin through a bakelite plate. (See reference 1.) In accordance with the graphical presentation in reference 1, K is plotted against $\frac{d}{P}$ rather than $\frac{d}{P - d}$.

DISCUSSION

At a value of rivet pitch P equal to the rivet diameter D, P − D becomes zero. Thus, no load can be carried by the joint, and the extrapolation of the constant fatigue life curves in figure 17 to zero load at P = 0.125 inch is justifiable. The establishment of these curves at the low values of load per rivet affords a means for extrapolating the curves of figure 18. The extrapolations, it will be noted, give optimum values of rivet pitch. These fall roughly between P = 0.25 inch and P = 0.4 inch for the range of fatigue life studied, and, on the basis of fatigue strength, justify the Lockheed Design Handbook Specification of 3D for minimum rivet spacing.

In making use of the results dealing with the effective stress concentration factor in fatigue K_F and in the interpretation of the curves of figure 23 and those that follow, it is necessary to define clearly K_F and to distinguish between it and the theoretical stress concentration factor K. If, owing to a rivet, a notch, or some other "stress raiser," an abnormal stress condition exists, then the ratio of the maximum stress intensity to that calculated by ordinary formulas is the theoretical stress concentration factor K, the changed distribution of stress being disregarded. The value of the maximum stress intensity, provided it does not exceed the elastic limit of the material, often can be determined mathematically, photoelastically, or by direct strain measurements. Where the fatigue strength of a single-row lap riveted joint is involved, the stress concentration factor may not be directly dependent upon the maximum stress intensity, but rather upon the combination of that maximum stress intensity with several other variables. Thus, rivet pitch, edge distance, distortion of the hole arising from upsetting the rivet, the surface condition and the heterogeneity of the metal, the plastic yielding in the region of the hole, and the orientation of the grain, all act with different effects: some to increase, and others to decrease the fatigue strength of the joint. The effective stress concentration factor in fatigue, as defined under Results is the measure of the over-all effect of these variables. It provides an adequate parameter in the evaluation of any of the above factors separately investigated, as is demonstrated in this paper for the case of rivet pitch and load. Furthermore, its use can be

extended to become a working index in the analysis and the comparison of all fatigue test results, the determination of the fatigue strength of airplane structures, and, ultimately, the design of these structures on the basis of life expectancy.

The results shown in figure 23 point to the existence of definite interrelationships among the fatigue life, the rivet pitch P, the maximum load per rivet, and the effective stress concentration factor in fatigue. As a further step toward defining these interrelations, figures 24 and 25 were developed in which the effective peak stress is plotted against nominal stress and rivet pitch, respectively. Here, again, the effective peak stress is not the maximum stress intensity actually present but the product of K_F and the nominal stress across the net width of the joint, and it is the measure of the combined effects produced by the variables previously enumerated. It is, by definition, equal to S_F, the maximum value of the cyclically varying stress that the material itself, without stress raisers, can withstand for any given number of cycles. Since, at zero value of nominal stress, the effective peak stress also must be zero, the curves of figure 24 all pass through the origin. Since for these curves the value of K_F for any particular magnitude of nominal stress is the ratio of the ordinate to the abscissa, a means is afforded of determining K_F for stresses lower than those experimentally considered.

The next logical step in our analysis is the development of the curves in figure 26. The extrapolations to zero load are obtained directly from figure 24; whereas the extensions to high loads are based on static test ultimates. The curves display the interesting fact that the variation of K_F is rapid at intermediate loads, much less pronounced at low loads, and negligible beyond 2/3 ultimate. This phenomenon doubtlessly can be attributed to the fact that plastic deformation, starting at very low loads, serves to minimize the concentration of stress in an increasing manner until at approximately 2/3 ultimate its effect becomes negligible.

The rapid change of K_F at intermediate loads is again shown in figure 27. Plotted as a family of constant load per rivet curves, it affords a means of determining the effective stress concentration factor in fatigue, for the joints tested, for any value of $\frac{d}{P-d}$ and any

loading between zero and ultimate load per rivet, and establishes a definite relationship between K_F and the ratio of the rivet diameter to the width of sheet between rivets.

The striking parallel between the two curves of figure 28 demonstrates the validity of the stress concentration factors determined by photoelastic analysis. These are, however, modified by plastic deformation, as has been previously brought out. The agreement shown between photoelastic and fatigue analysis should be regarded with care, for, whereas Frocht and Hill used a close-fitting pin loaded in double shear, the results of this paper are based upon a specimen in which an upset rivet in single shear actually enlarges and distorts the hole. It appears, nevertheless, that the use of photoelastic analysis for predicting maximum values of K_F may be of great importance and should be more thoroughly investigated.

The decrease of the effective stress concentration factor in fatigue with increasing load leads to some interesting hypotheses.

It has been shown in tests, especially on steels, that the harmful effect of any stress raiser is increased as the hardness of the steel is increased, until the endurance limit for severely notched specimens may be actually lower for very hard than for moderately hard steels. In the light of what has been found here, the explanation that immediately presents itself is that, for nominal stresses at the endurance limit, the hard steel in the region of the stress raiser has undergone little or no plastic deformation, and, consequently, little or no decrease in the effective peak stress takes place. In the case of soft steel, yielding may take place to decrease appreciably the effective peak stress and, by the same token, to provide the beneficial effects of prestretching and moderate overstressing on the fatigue strength of structures containing stress raisers.

It may be said generally that the results given in this report appear to bear out the useful function of plasticity in permitting sufficient deformation of the more highly stressed fibers, in a nonuniformly stressed article, to bring about a more favorable distribution of stress. And, further, as has been brought out previously, there appears to be a limit to the usefulness of this plasticity, depending upon the structure and the magnitude of the stresses involved.

CONCLUSIONS

1. For the R value and the type of joint tested:

a) The fatigue strength per rivet increases with increasing rivet pitch P at least to P = 1.5 inches.

b) The greatest fatigue strength per linear inch of joint is obtained for values of P between 0.25 inch and 0.4 inch.

c) The effective peak stress increases with rivet pitch.

d) The effective stress concentration factor in fatigue varies inversely as the load.

2. For low stresses the possibility presents itself of predicting, on the basis of photoelastic analysis, the values of the effective stress concentration factor in fatigue.

3. The usefulness of plasticity in decreasing the peak stresses in a nonuniformly stressed part is indicated. From this, it follows that the use of materials with high ratios of yield strength to ultimate strength may actually result in lowered fatigue strengths. Since tests have been started on joints of secondary heat-treated material, this point will be established in the very near future.

Lockheed Aircraft Corporation,
Burbank, Calif., Nov. 7, 1942.

APPENDIX

Since no fatigue data at the desired range ratio was available for 24S-T alclad sheet, the curves shown in figures A-1 and A-2 were established by means of tests run in a Lockheed fatigue testing machine. The principal dimensions of the test specimen are shown in figure A-3, the drawing of the die from which the specimens were manufactured. The test setup is shown in figure A-4.

Standard X-1009 tensile coupons were cut from the sheets used for making the fatigue specimens and tested in the Triplett and Barton 300,000-pound testing machine with the following results:

Specimen	Ultimate stress (lb/sq in.)	Yield stress (lb/sq in.)	Percent elongation (2-in. gage length)
1	66,200	51,100	19
2	66,500	51,100	19½
3	66,700	51,400	18½
4	63,600	51,000	19

REFERENCE

1. Frocht, M. M., and Hill, H. N.: Stress-Concentration Factors around a Central Circular Hole in a Plate Loaded through a Pin in the Hole. A.S.M.E. Jour. of Appl. Mech., March 1940, pp. 5-9. illus.

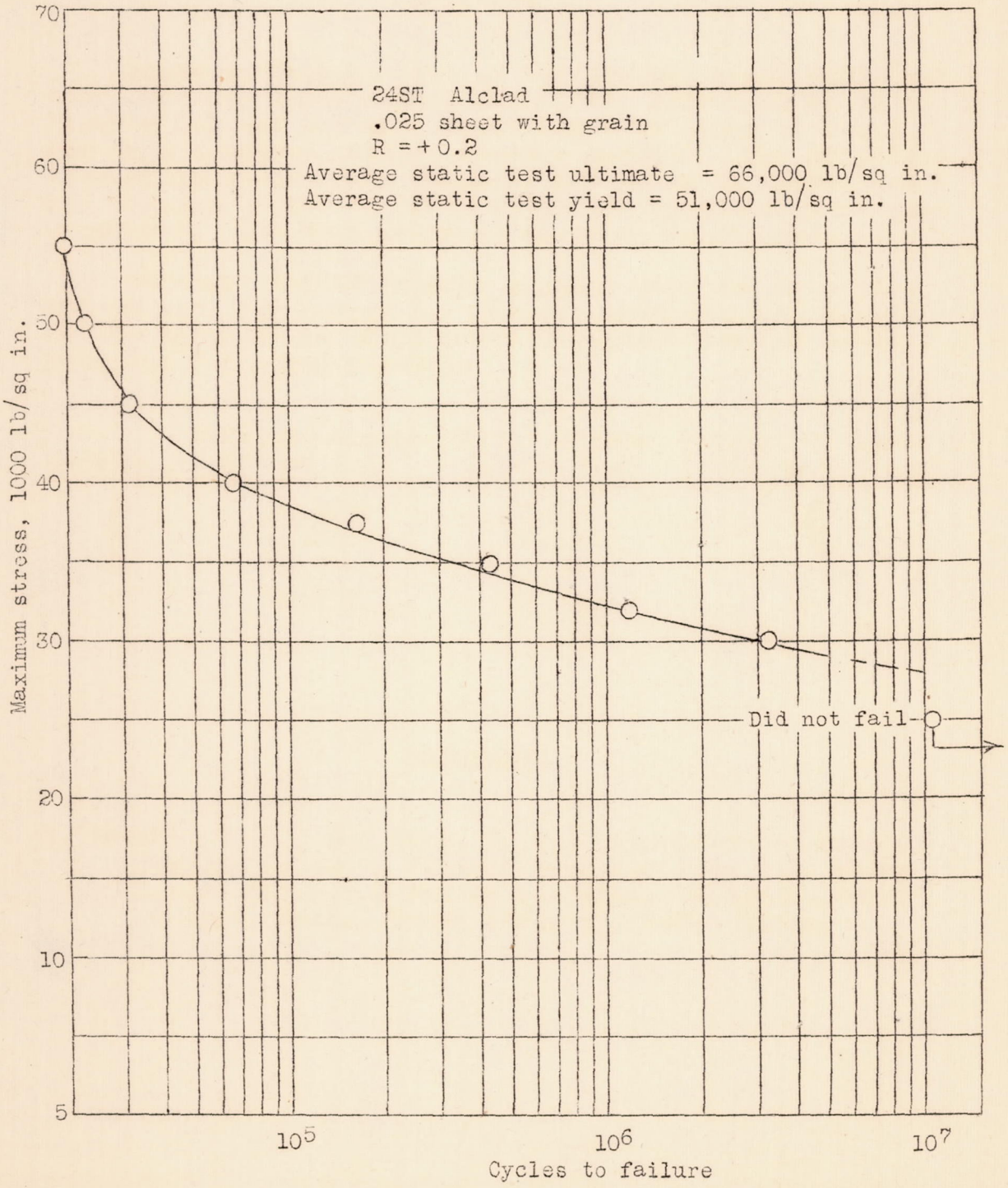

Figure A-1.- Axial tension fatigue curve.

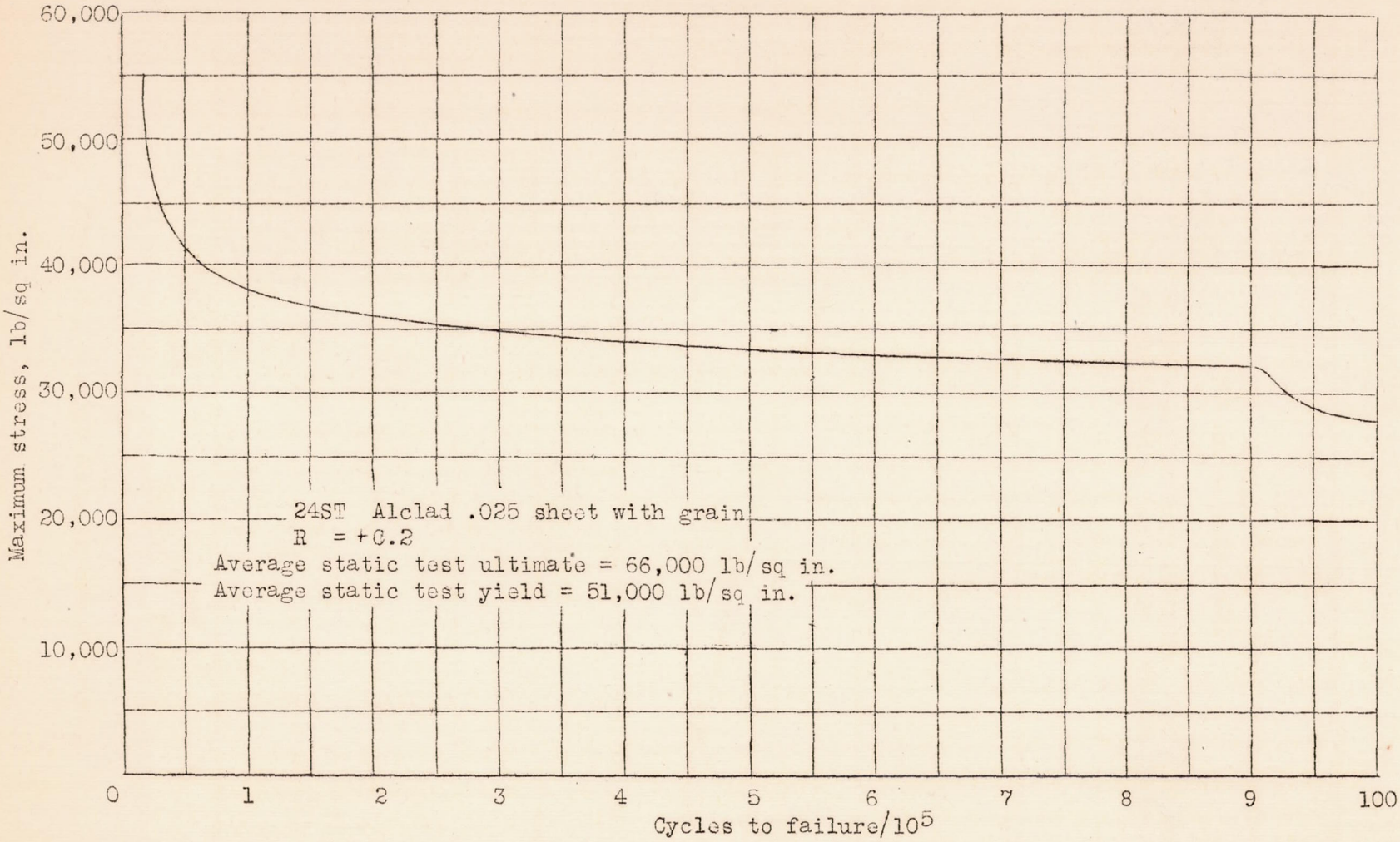

Figure A-2.- Axial tension fatigue curve.

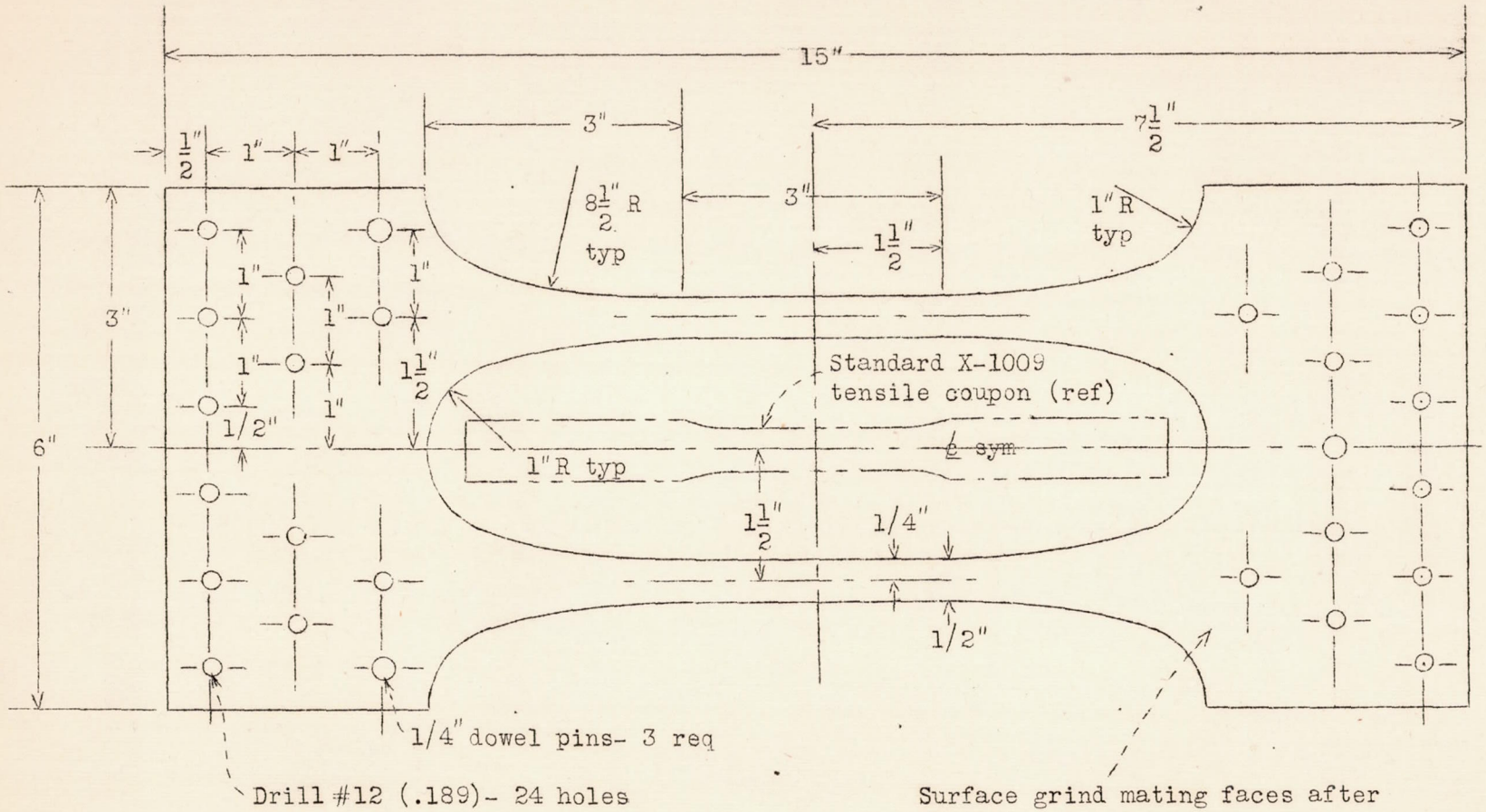

Note.-
1. Make from 3/8" Ketos die steel or equivalent
2. Heat treat to Rockwell C55
3. Smooth machine finish
4. 2 mating halves required
5. Grind edges to size after heat treatment

(Scale 1/2 size)

Figure A-3.- Jig-fatigue test specimen.

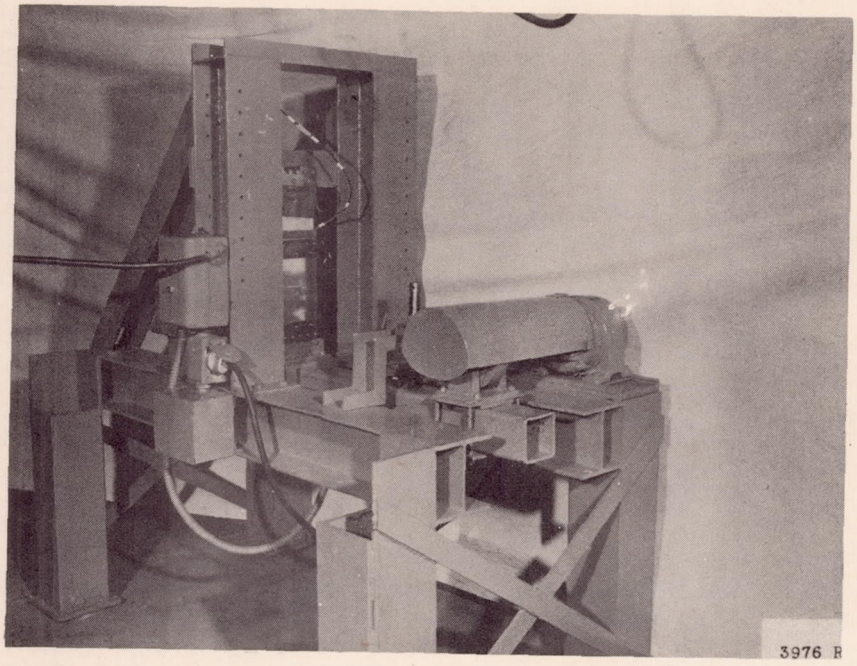

Figure 1.- Fatigue machine in operation.

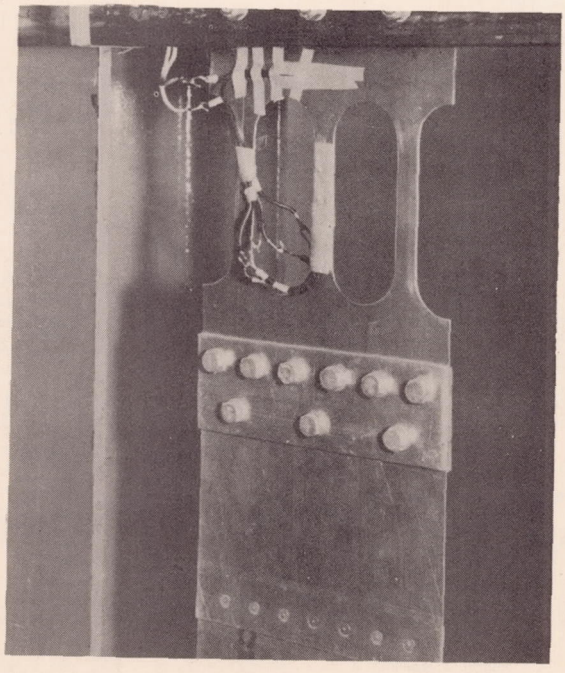

Figure 2.- Specimen mount with strain gauges.

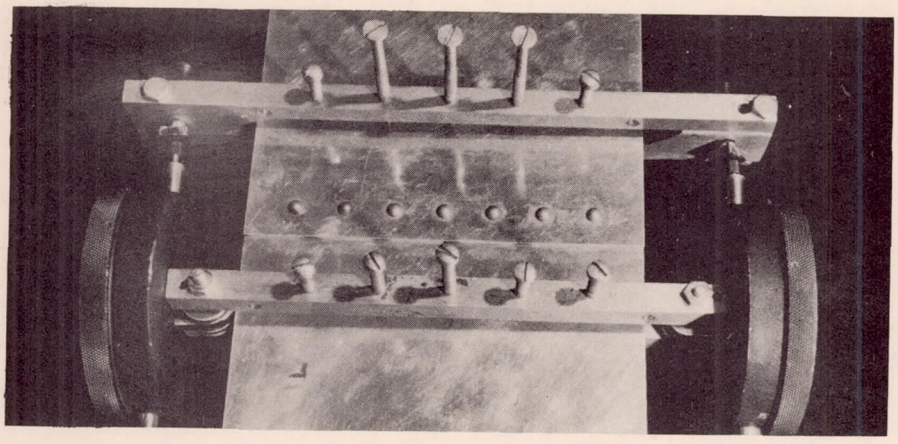

Figure 3.- Set up for obtaining load deformation data.

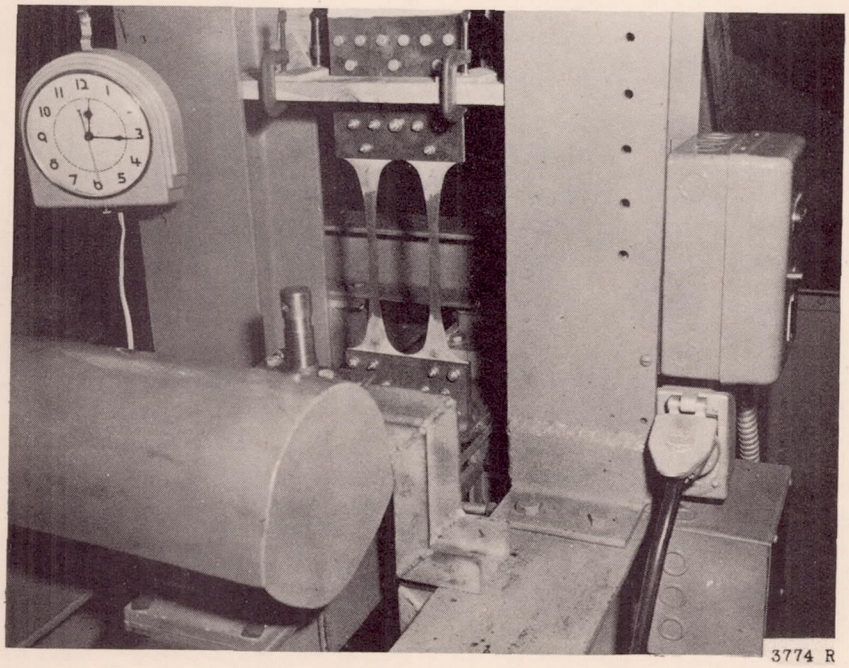

Figure A-4.

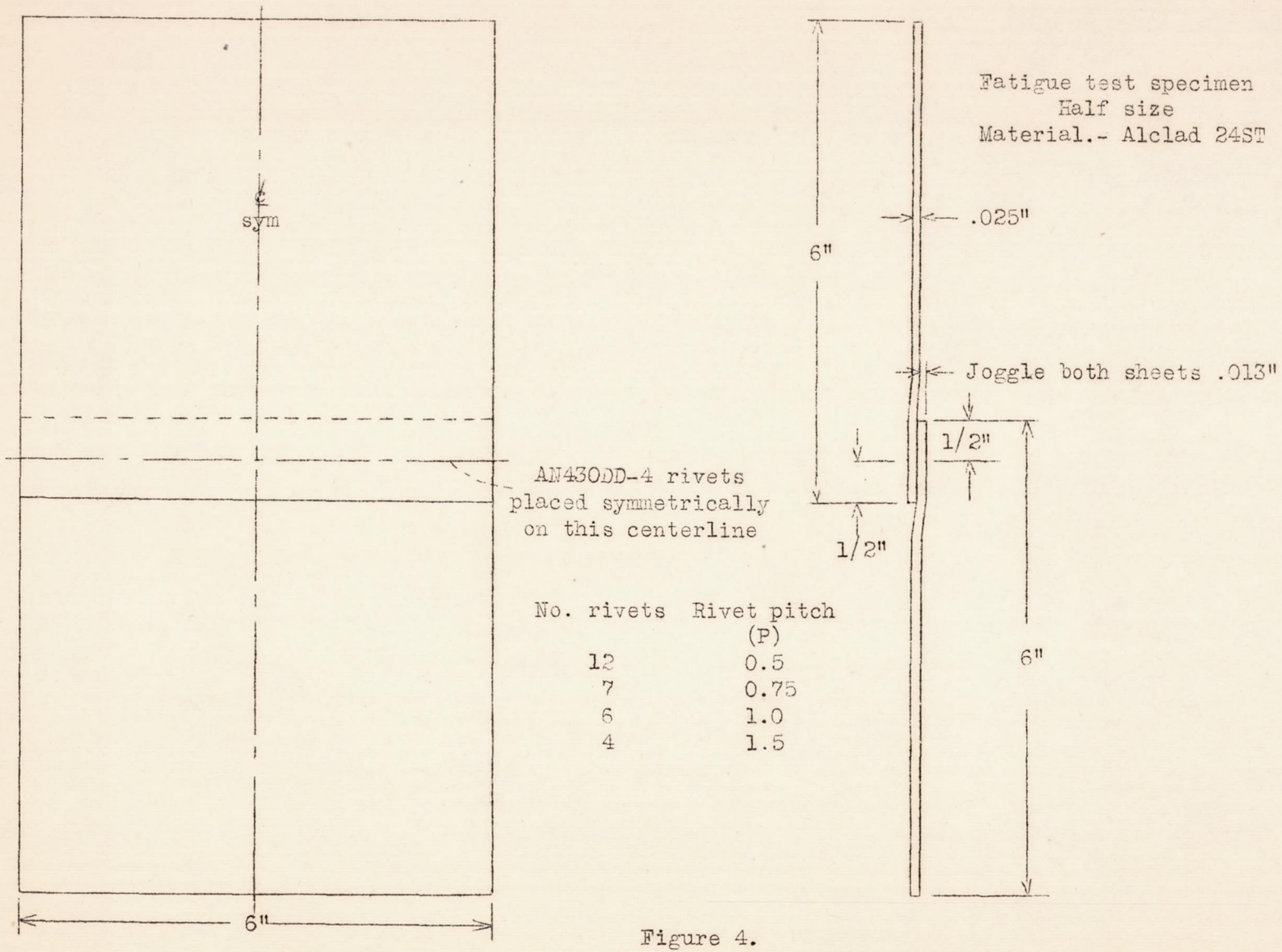

No. rivets	Rivet pitch (P)
12	0.5
7	0.75
6	1.0
4	1.5

Figure 4.

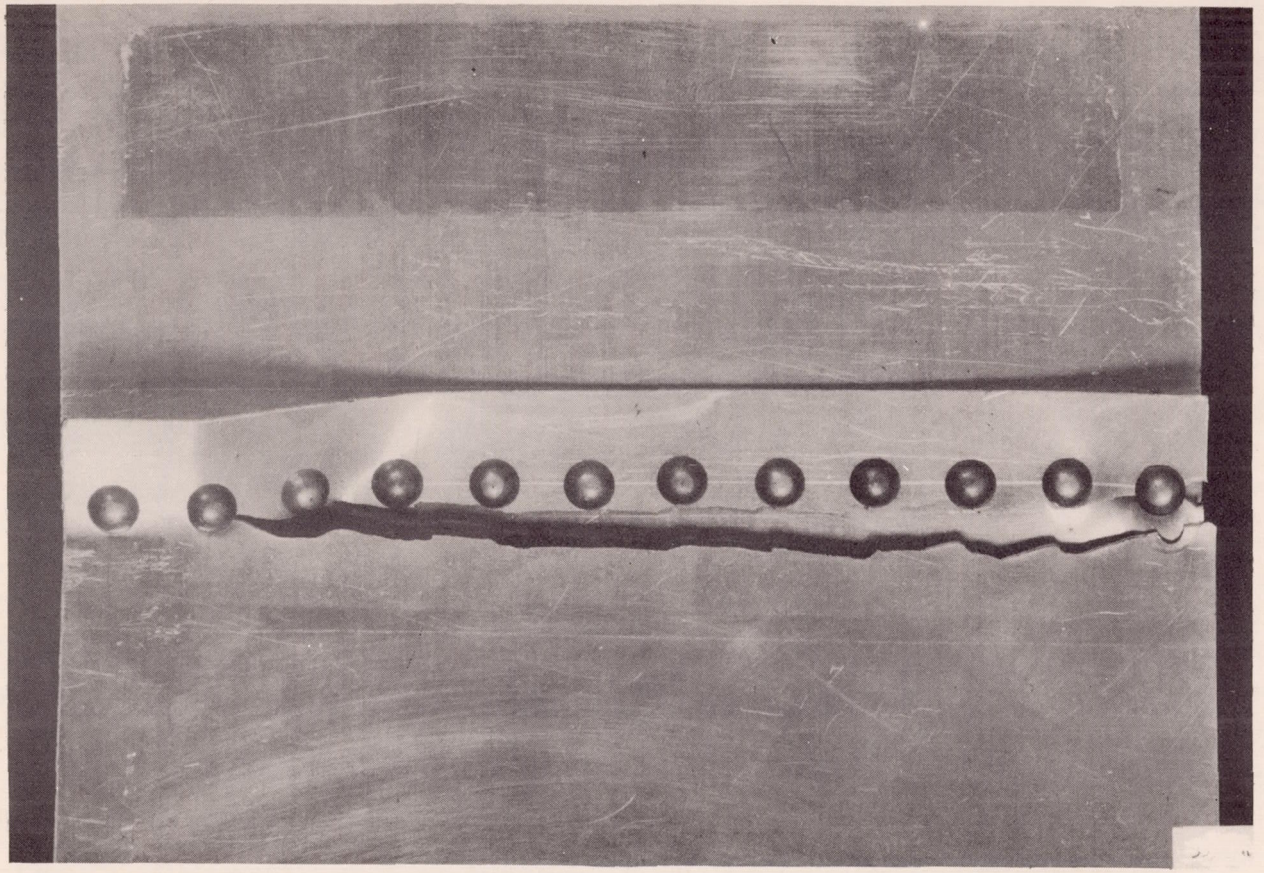

Figure 5.- Showing failure of specimen with P = 0.5 inch. Maximum load, 75 pounds/rivet, 150 pounds/linear inch; Cycles to failure, 2,670,000.

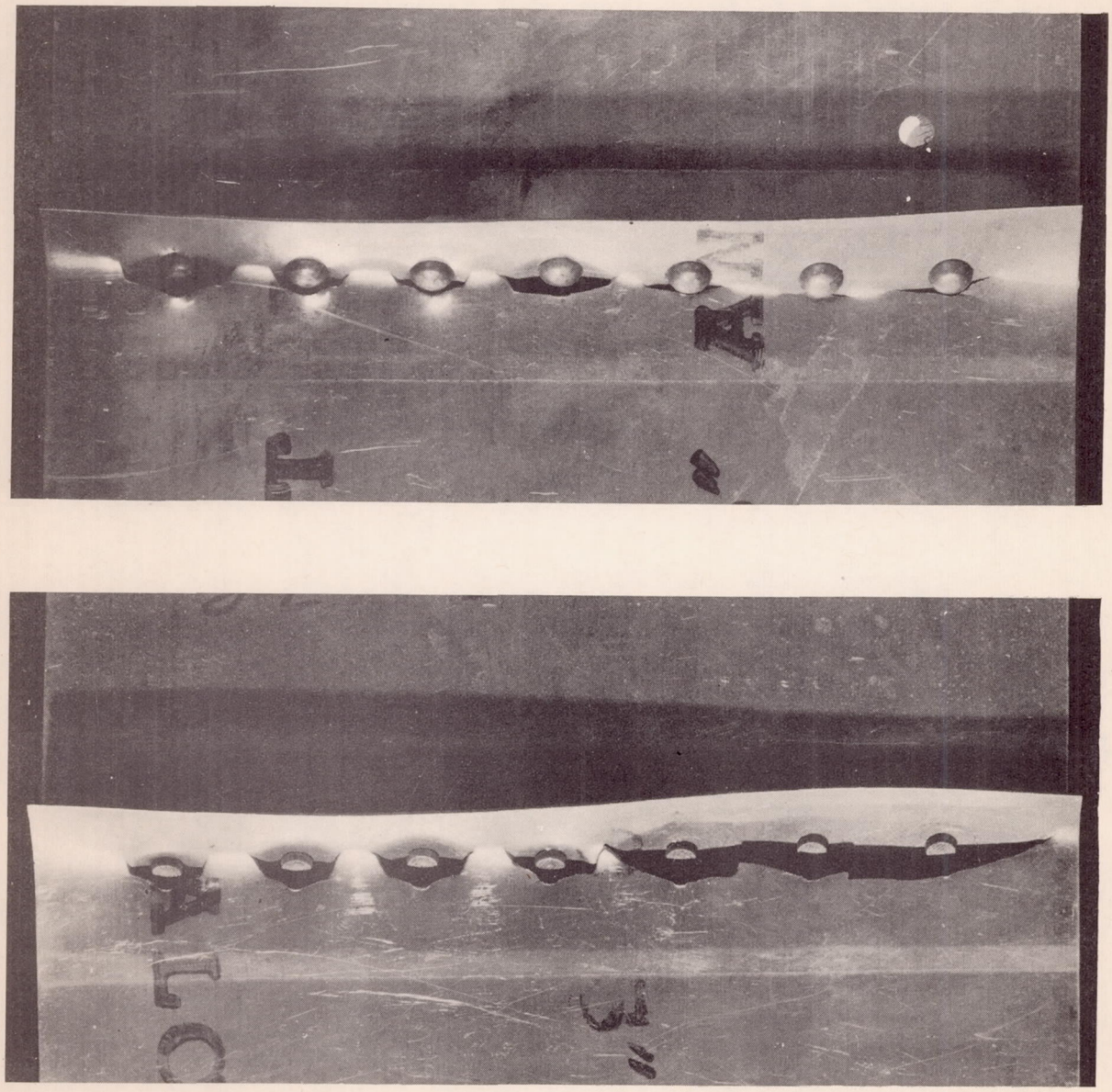

Figure 6.- Showing failure of each sheet of specimen with P = 0.75 in. Maximum load, 125 pounds/rivet, 146 pounds/linear inch; Cycles to failure, 115,000.

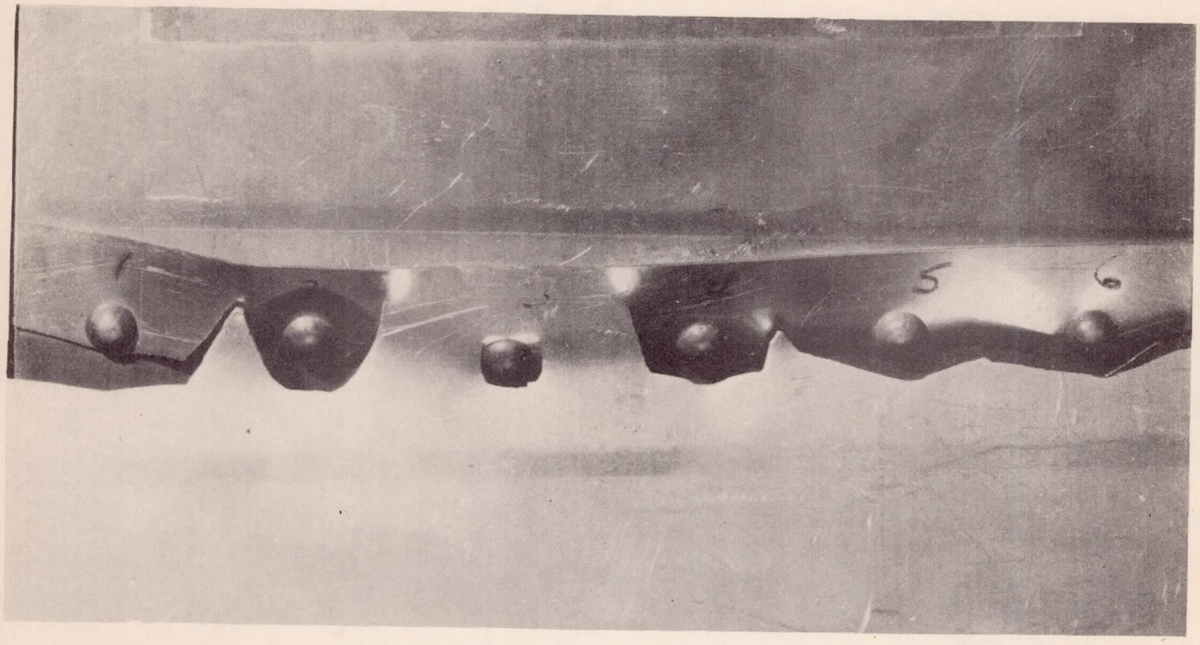

Figure 7.- Showing failure of specimen with P = 1.0 inch. Maximum load, 100 pounds/rivet, 100 pounds/linear inch; Cycles to failure, 4,330,000.

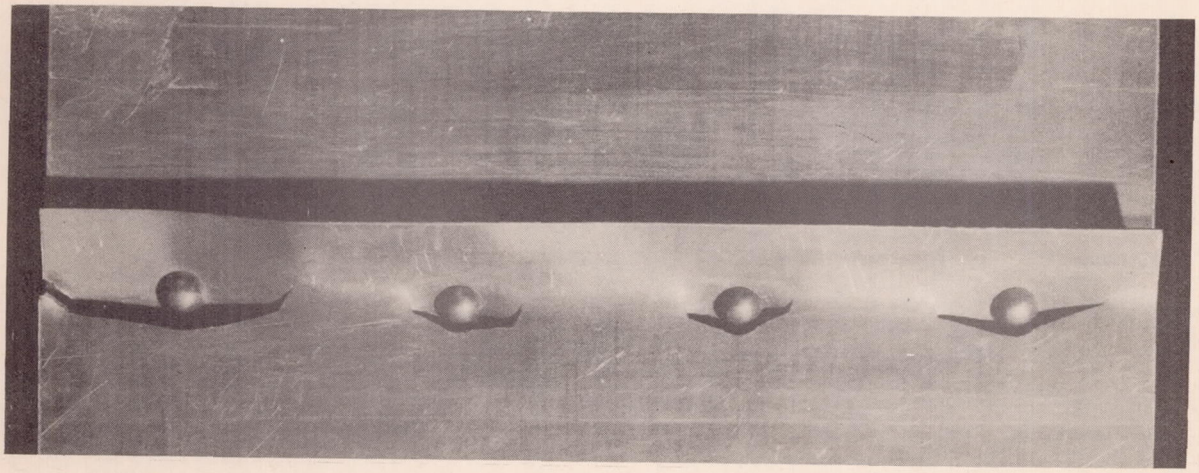

Figure 8.- Showing failure of specimen with P = 1.5 inch. Maximum load, 131 pounds/rivet, 87.5 pounds/linear inch; Cycles to failure, 4,050,000.

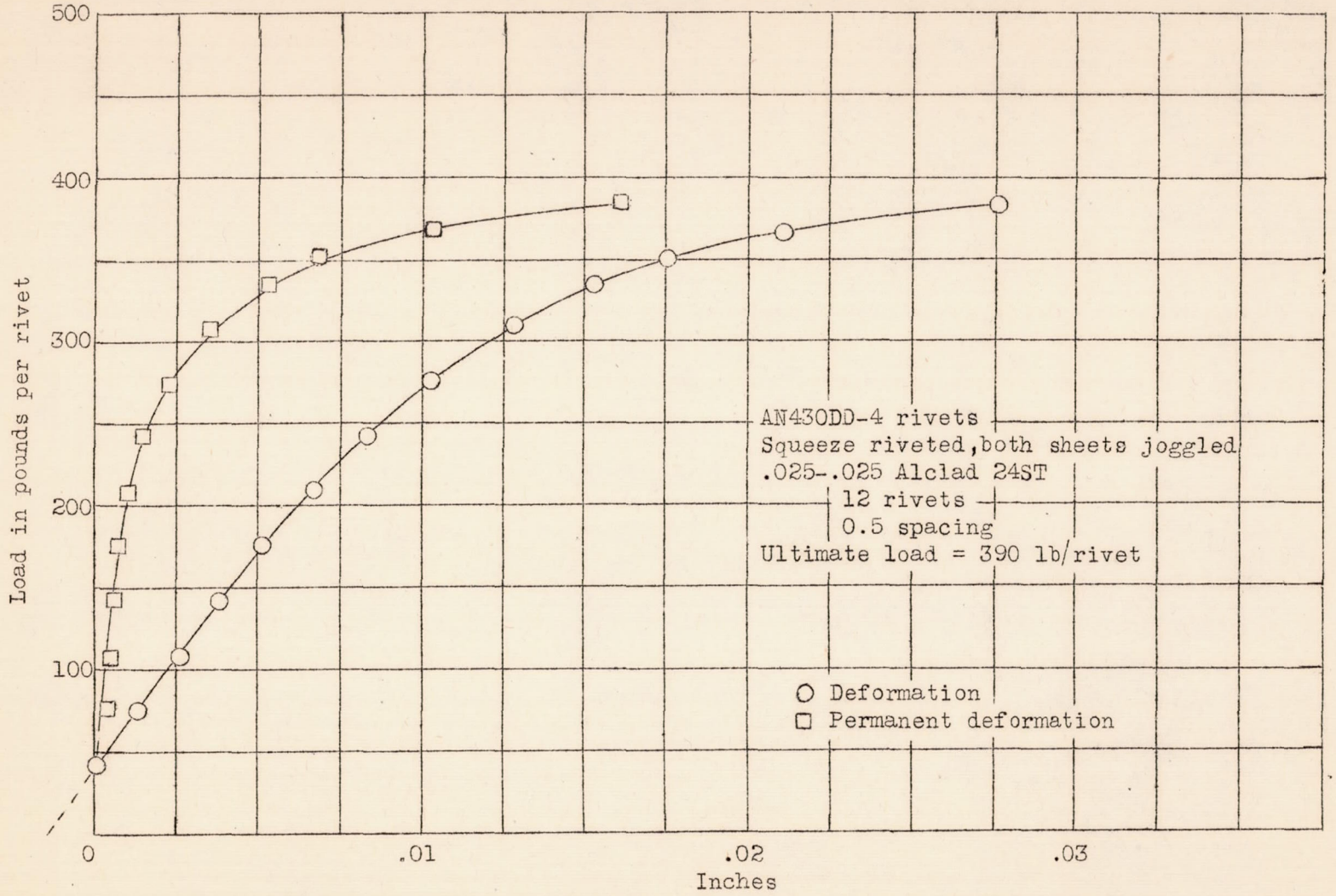
500
400
300
200
100
0
.01
.02
.03
Inches
Load in pounds per rivet
AN430DD-4 rivets
Squeeze riveted, both sheets joggled
.025-.025 Alclad 24ST
12 rivets
0.5 spacing
Ultimate load = 390 lb/rivet
Deformation
Permanent deformation

Figure 9.

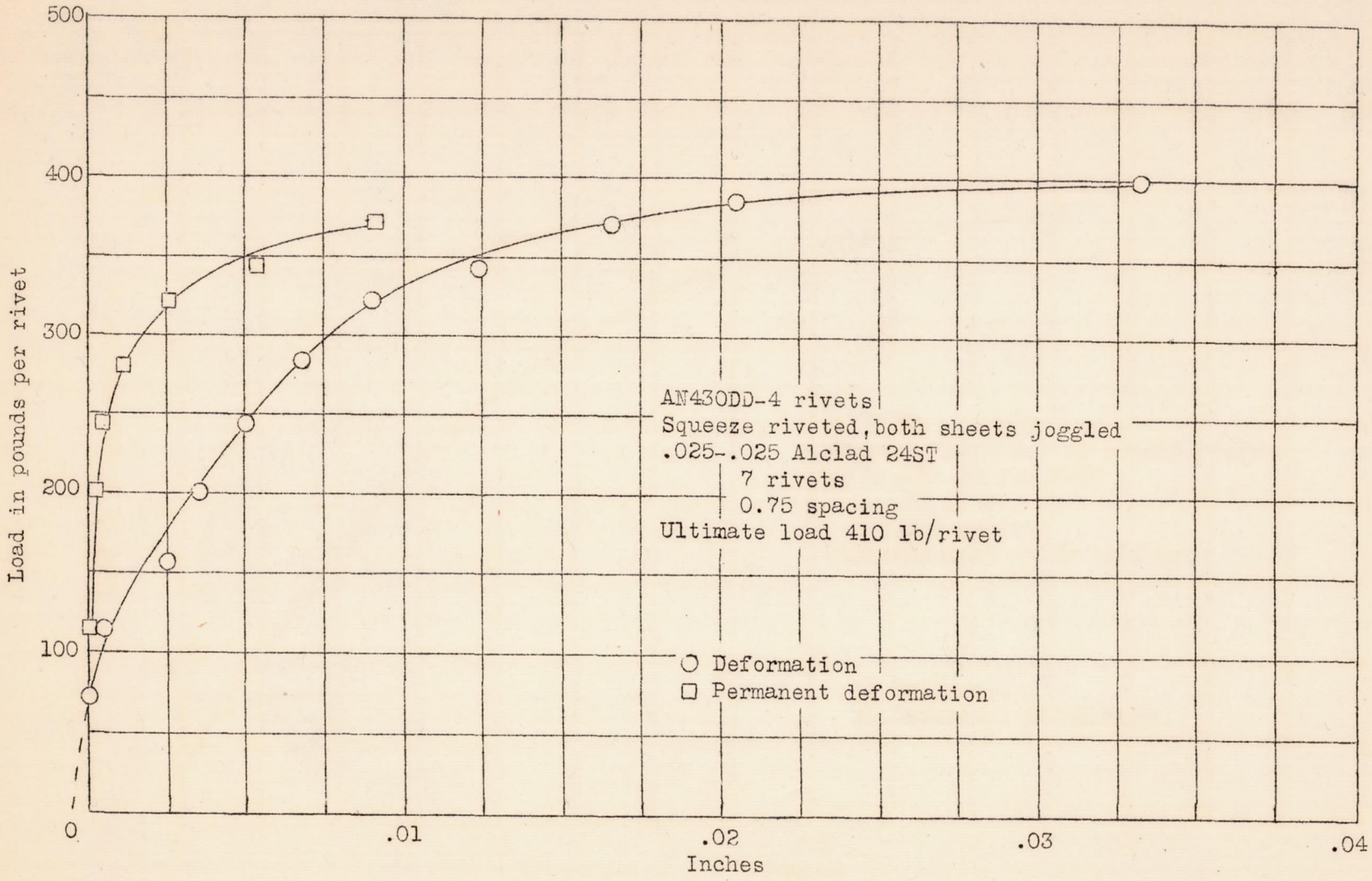
500
400
300
200
100
0
Load in pounds per rivet
.01
.02
.03
.04
Inches
AN430DD-4 rivets
Squeeze riveted, both sheets joggled
.025-.025 Alclad 24ST
7 rivets
0.75 spacing
Ultimate load 410 lb/rivet
Deformation
Permanent deformation

Figure 10.

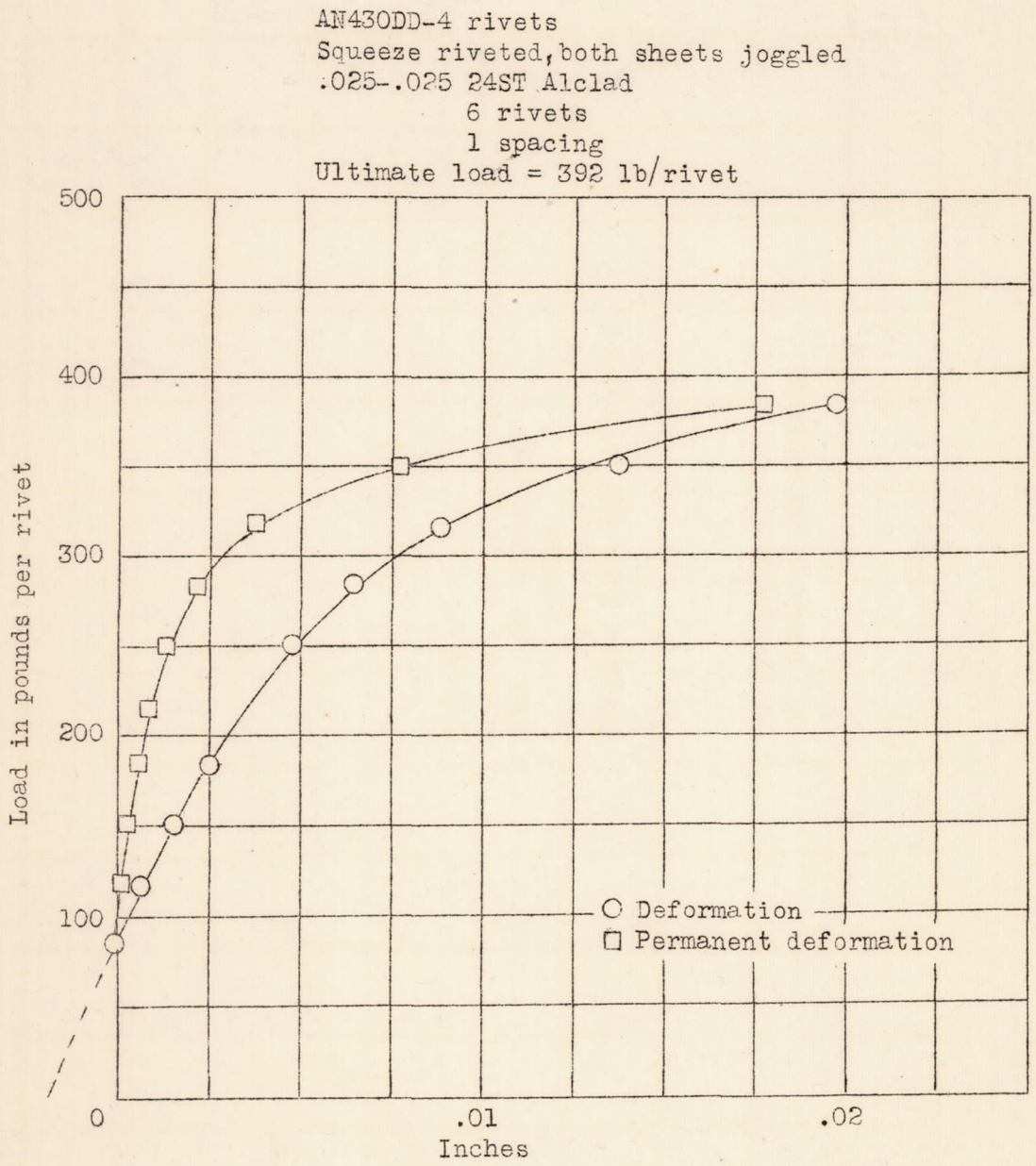
AN430DD-4 rivets
Squeeze riveted, both sheets joggled
.025-.025 24ST Alclad
6 rivets
1 spacing
Ultimate load = 392 lb/rivet
500
400
300
200
100
0
Load in pounds per rivet
.01
.02
Inches
Deformation
Permanent deformation

Figure 11.

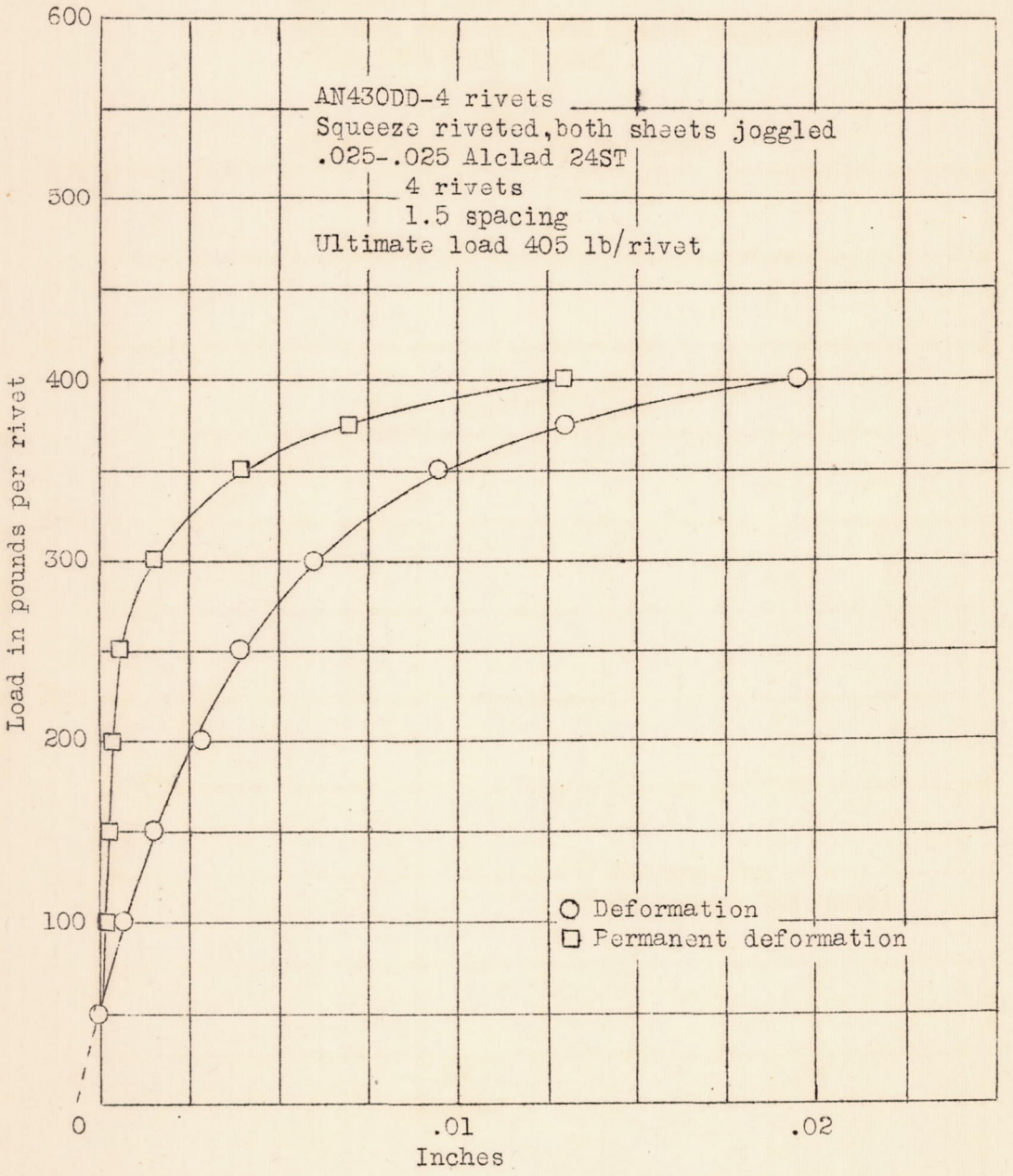
AN430DD-4 rivets
Squeeze riveted, both sheets joggled
.025-.025 Alclad 24ST
4 rivets
1.5 spacing
Ultimate load 405 lb/rivet
Load in pounds per rivet
600
500
400
300
200
100
0
.01
.02
Inches
Deformation
Permanent deformation

Figure 12.

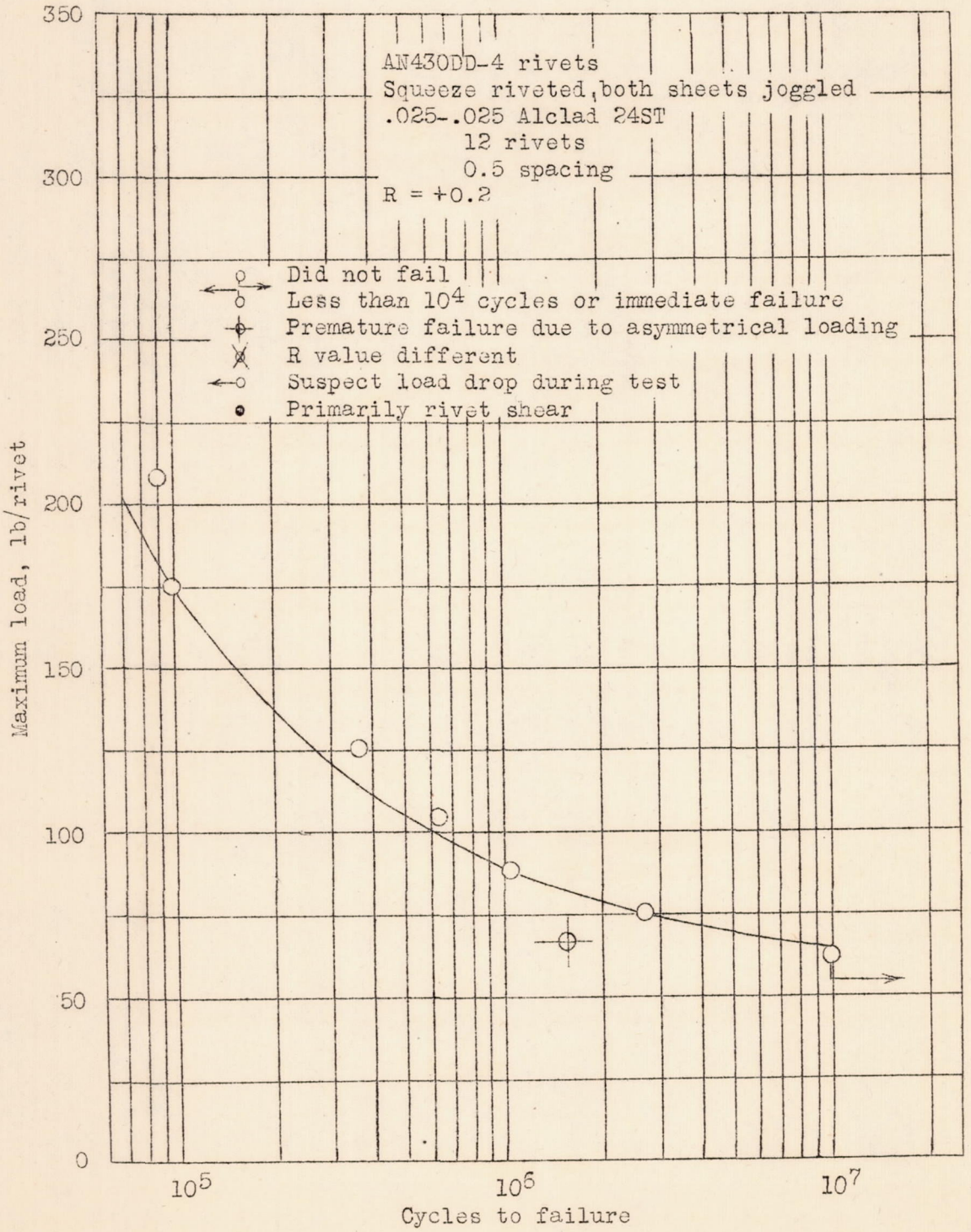
AN430DD-4 rivets
Squeeze riveted, both sheets joggled
.025-.025 Alclad 24ST
12 rivets
0.5 spacing
R = +0.2
Did not fail
Less than 10^4 cycles or immediate failure
Premature failure due to asymmetrical loading
R value different
Suspect load drop during test
Primarily rivet shear
Maximum load, lb/rivet
350
300
250
200
150
100
50
0
10^5
10^6
10^7
Cycles to failure

Figure 13.

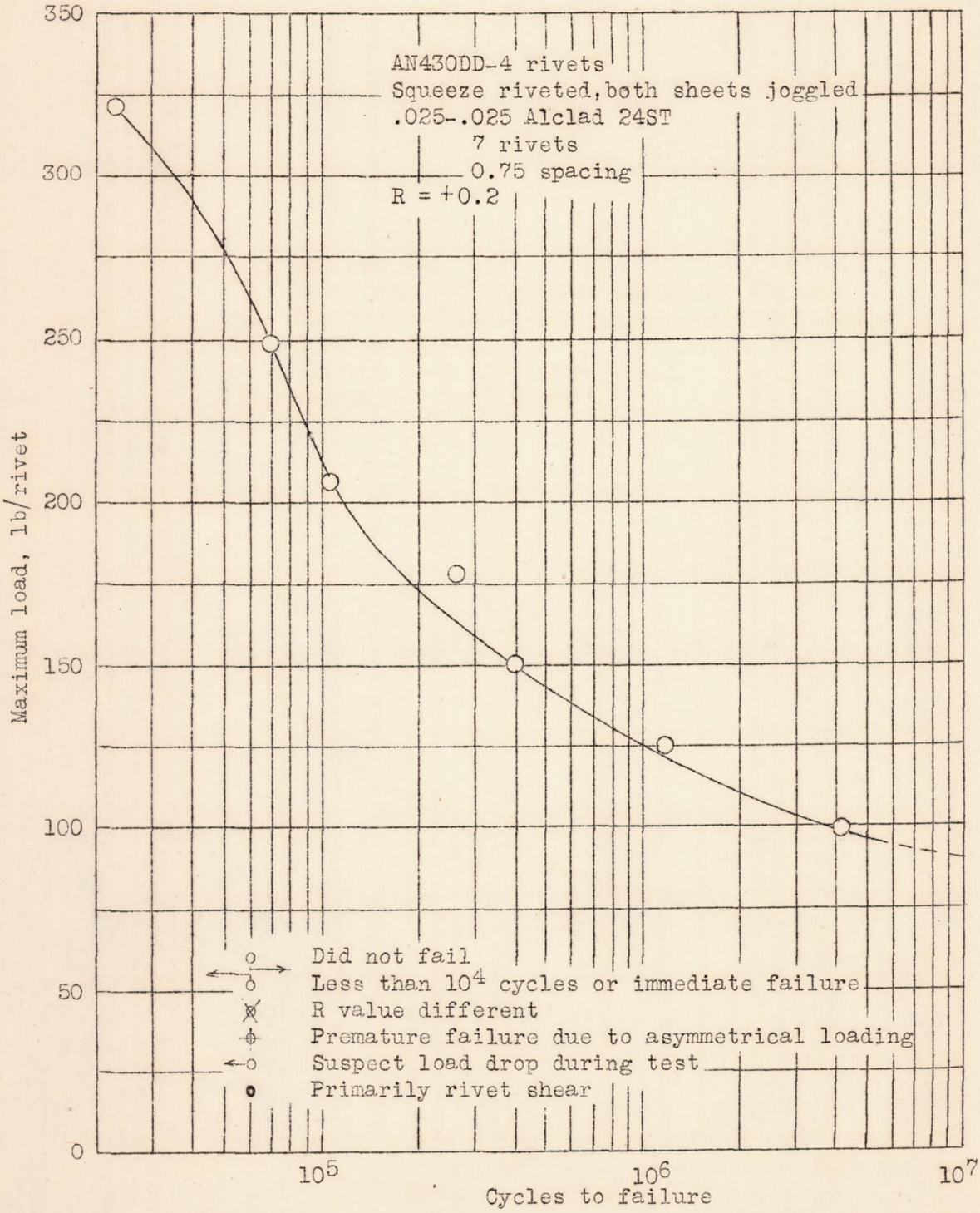
AN430DD-4 rivets
Squeeze riveted, both sheets joggled
.025-.025 Alclad 24ST
7 rivets
0.75 spacing
R = +0.2
Maximum load, lb/rivet
350
300
250
200
150
100
50
0
10^5
10^6
10^7
Cycles to failure
Did not fail
Less than 10^4 cycles or immediate failure
R value different
Premature failure due to asymmetrical loading
Suspect load drop during test
Primarily rivet shear

Figure 14.

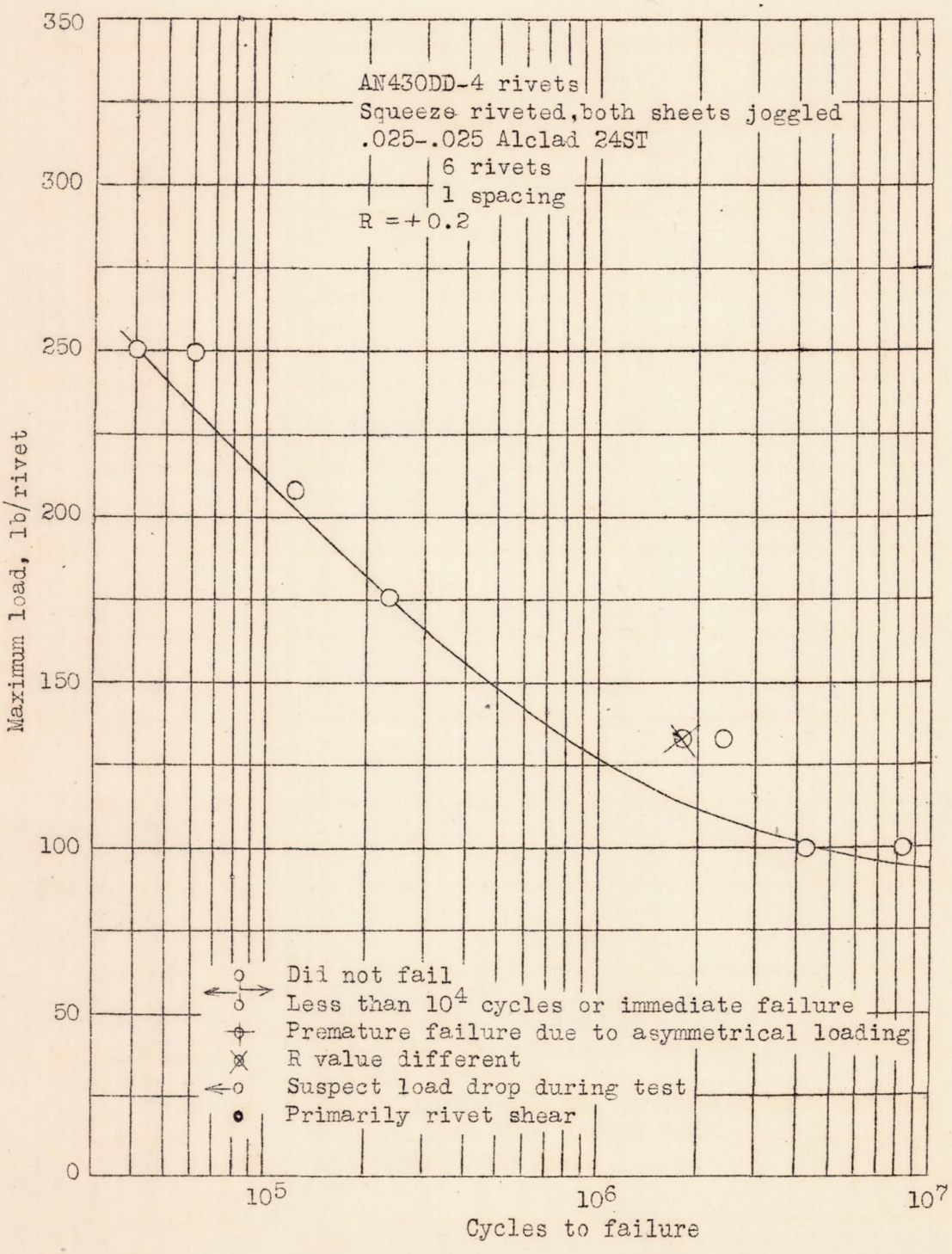
AN430DD-4 rivets
Squeeze riveted, both sheets joggled
.025-.025 Alclad 24ST
6 rivets
1 spacing
R = +0.2
Maximum load, lb/rivet
350
300
250
200
150
100
50
0
10^5
10^6
10^7
Cycles to failure
Did not fail
Less than 10^4 cycles or immediate failure
Premature failure due to asymmetrical loading
R value different
Suspect load drop during test
Primarily rivet shear

Figure 15.

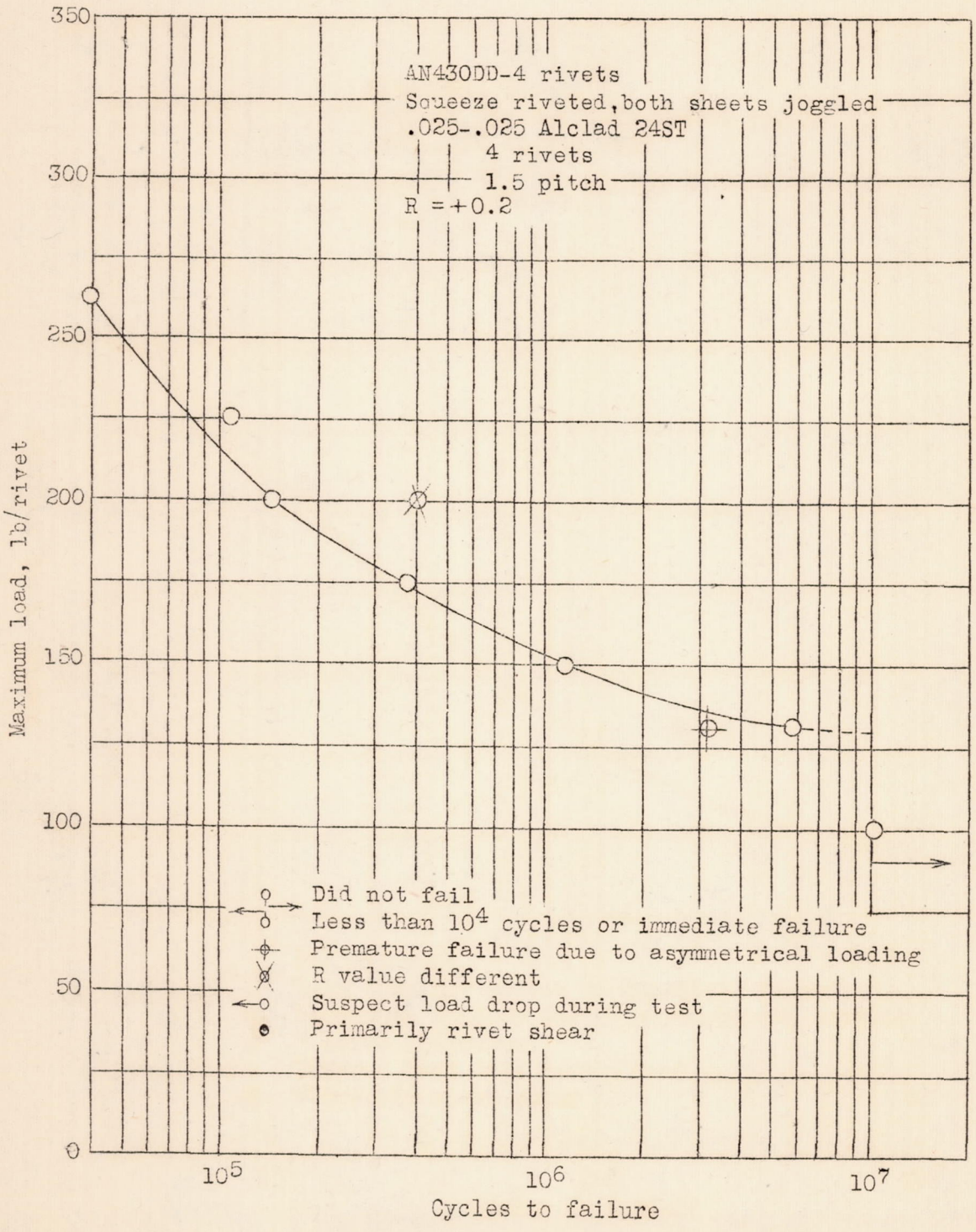
AN430DD-4 rivets
Squeeze riveted, both sheets joggled
.025-.025 Alclad 24ST
4 rivets
1.5 pitch
R = +0.2
Maximum load, lb/rivet
350
300
250
200
150
100
50
0
10^5
10^6
10^7
Cycles to failure
Did not fail
Less than 10^4 cycles or immediate failure
Premature failure due to asymmetrical loading
R value different
Suspect load drop during test
Primarily rivet shear

Figure 16.

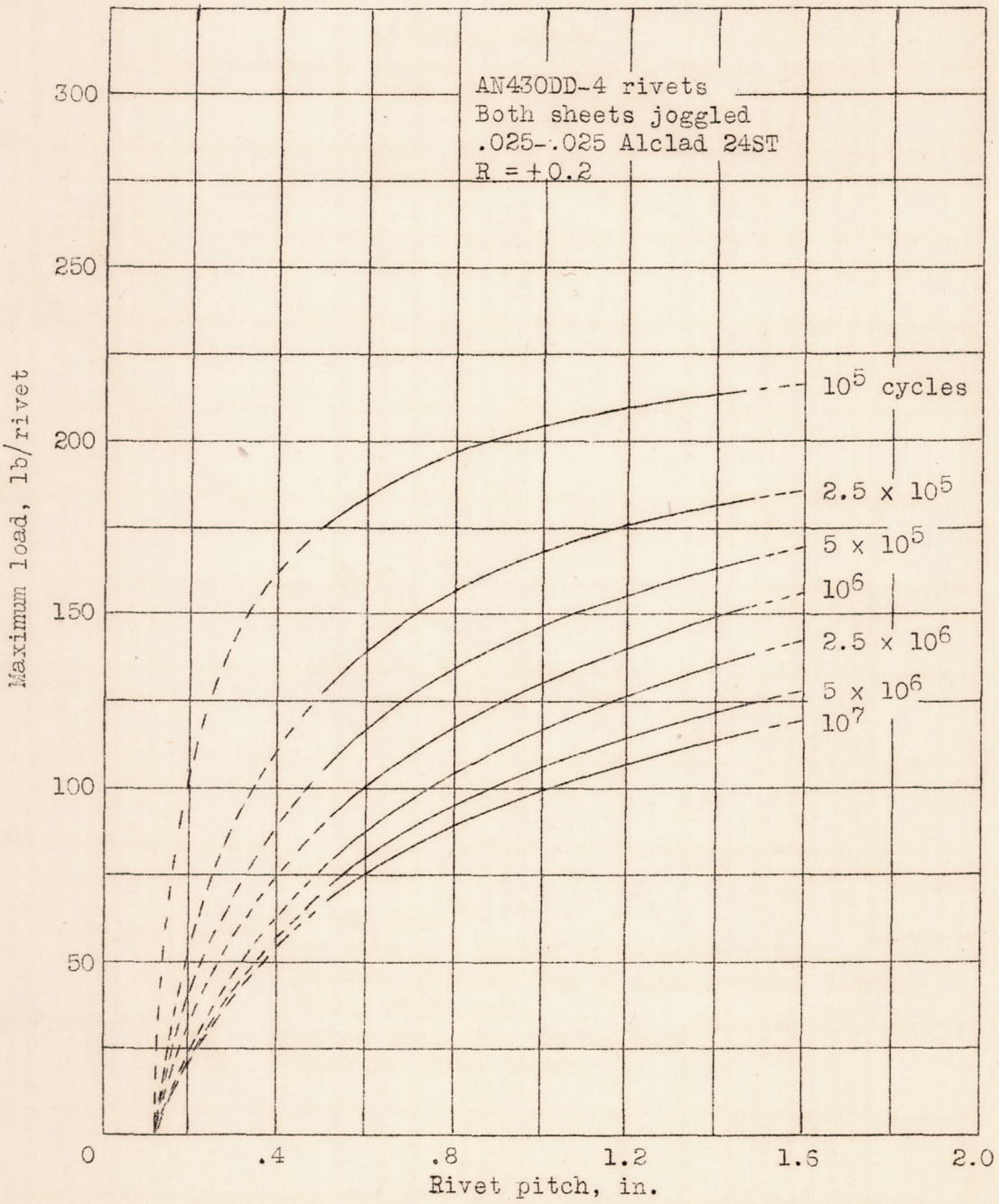

Figure 17.- Constant fatigue life curves.

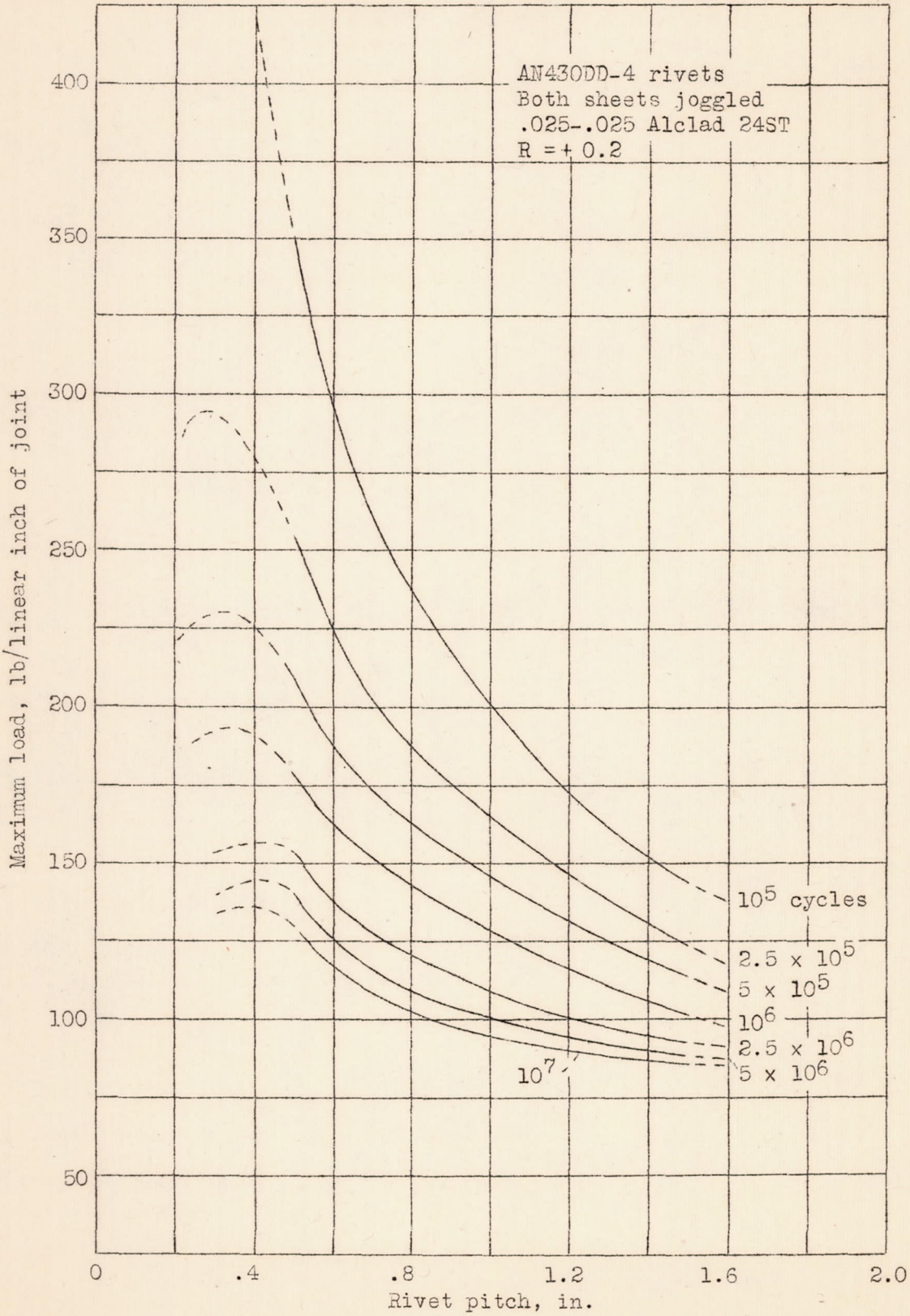

Figure 18.- Constant fatigue life curves.

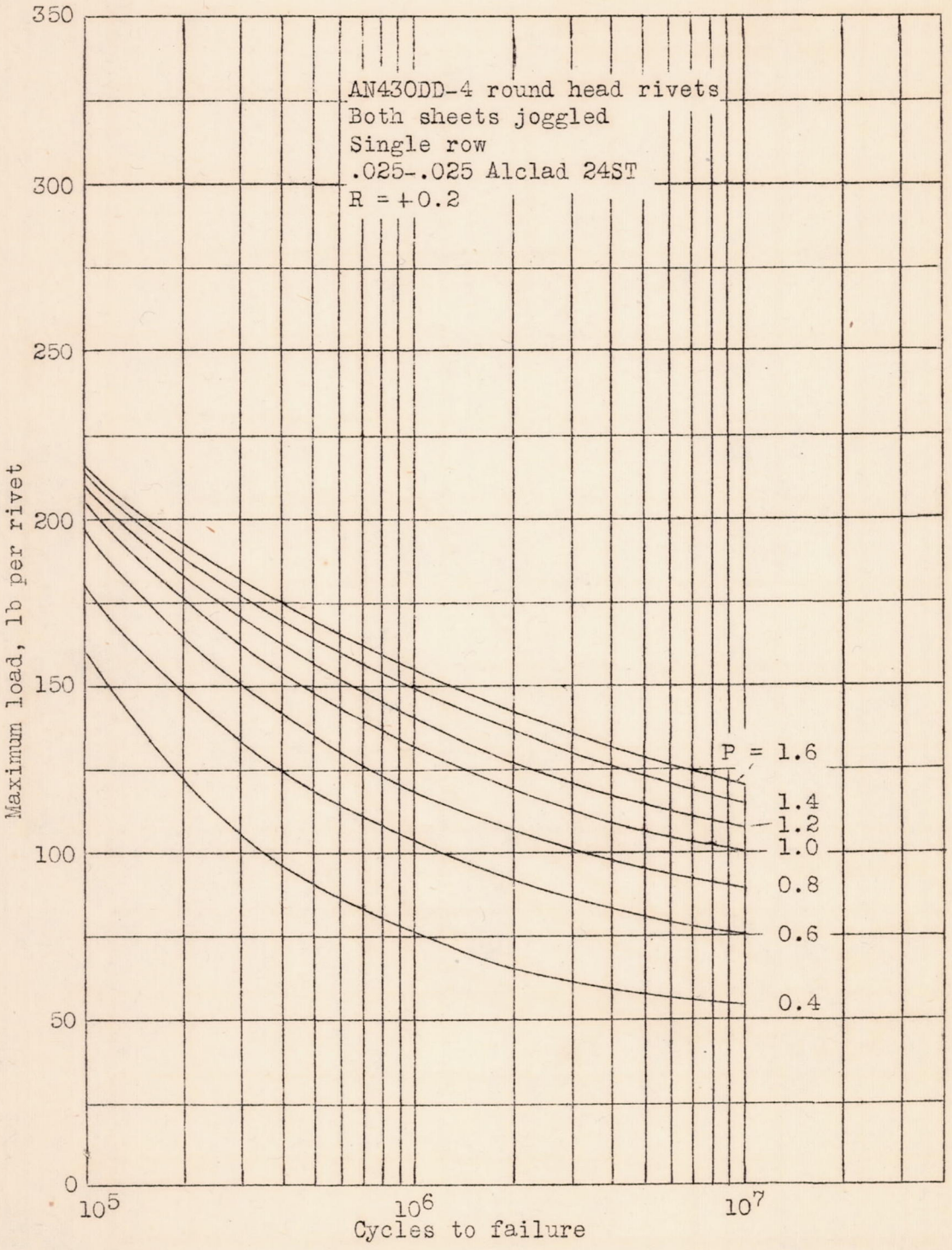

Figure 19.- Effect of rivet pitch upon fatigue strength, interpolated curves.

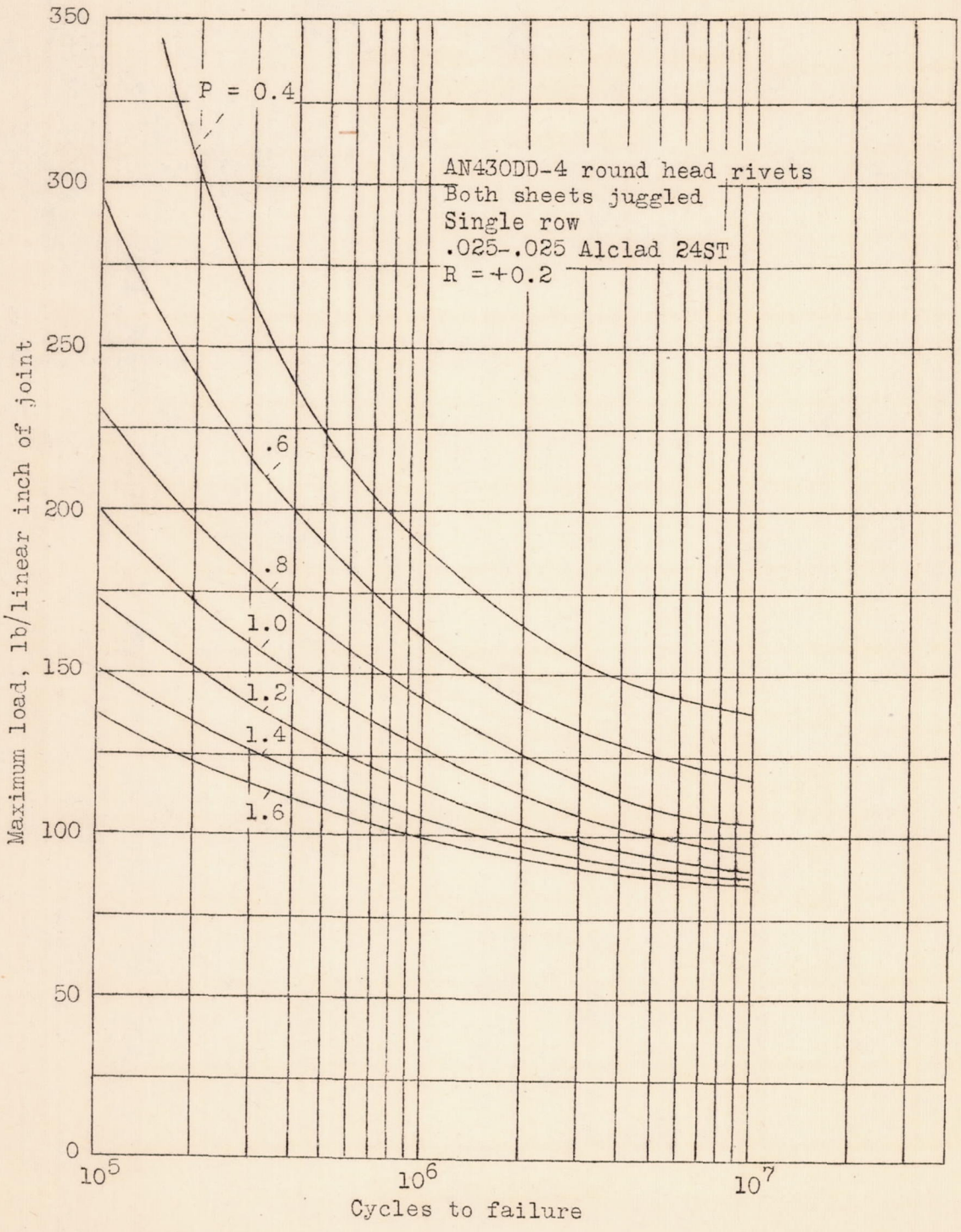

Figure 20.- Effect of rivet pitch upon fatigue strength, interpolated curves.

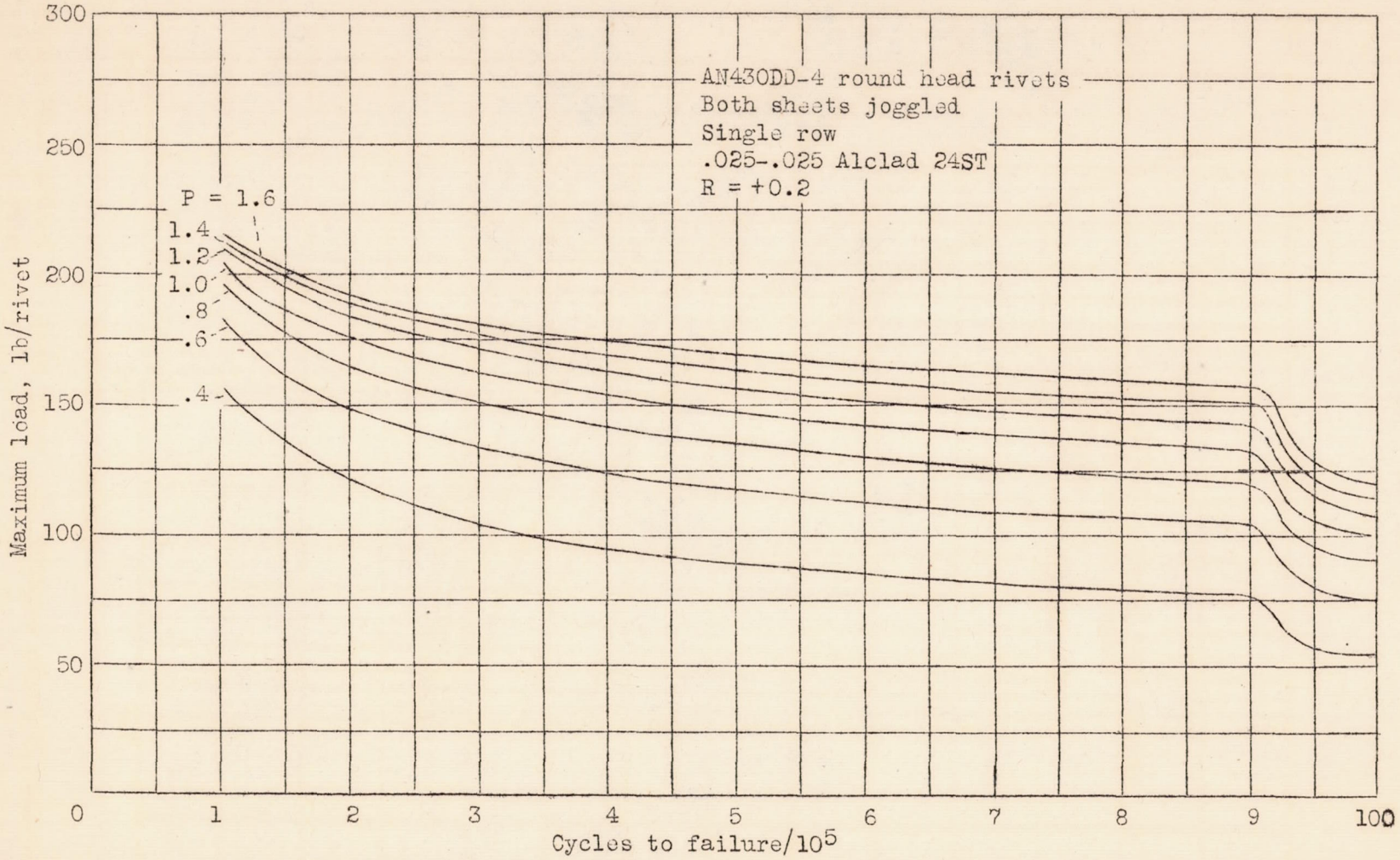

Figure 21.- Effect of rivet pitch upon fatigue strength, interpolated curves.

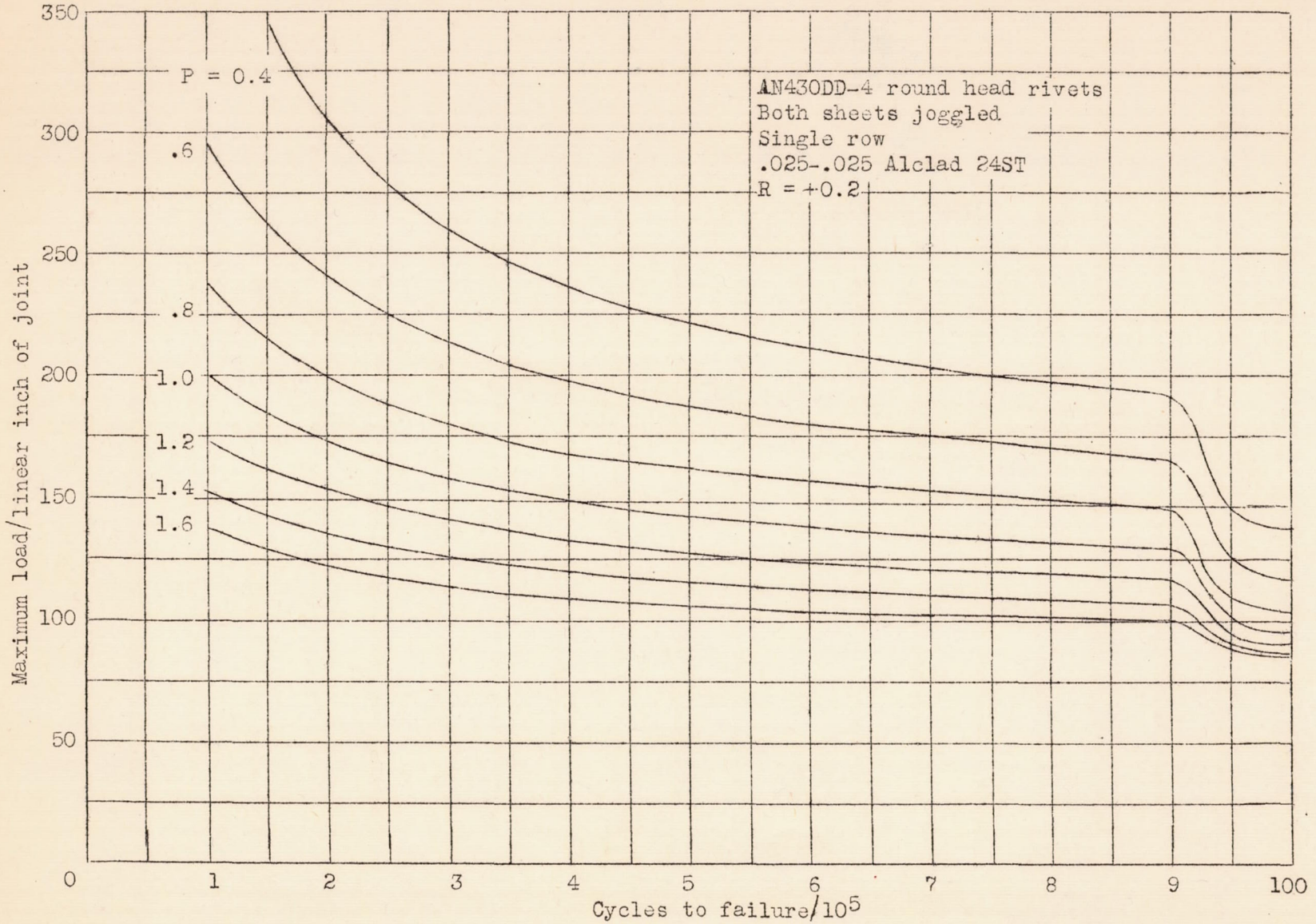

Figure 22.- Effect of rivet spacing upon fatigue strength, interpolated curves.

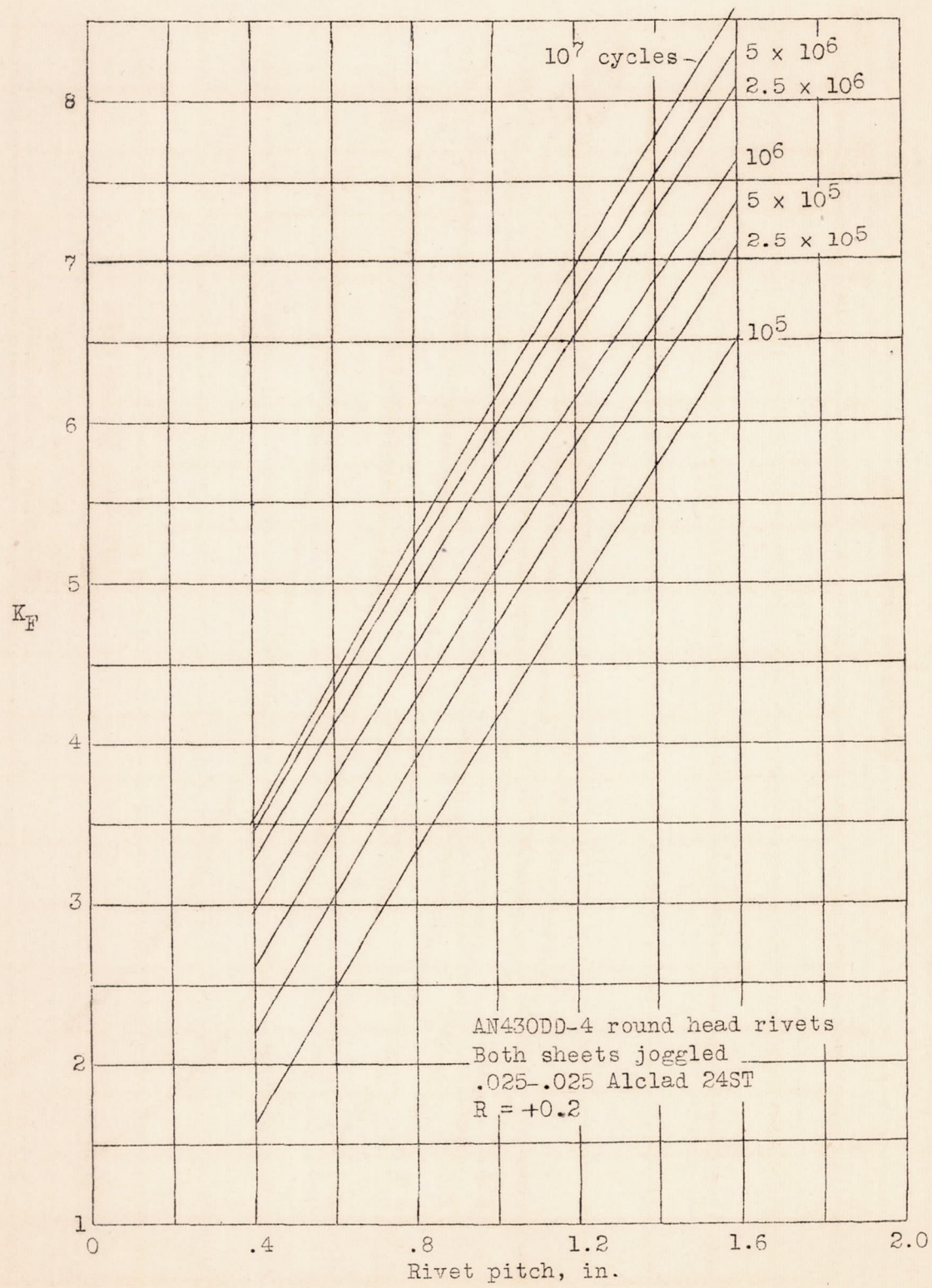

Figure 23.- Effect of rivet pitch upon the effective stress concentration factor in fatigue.

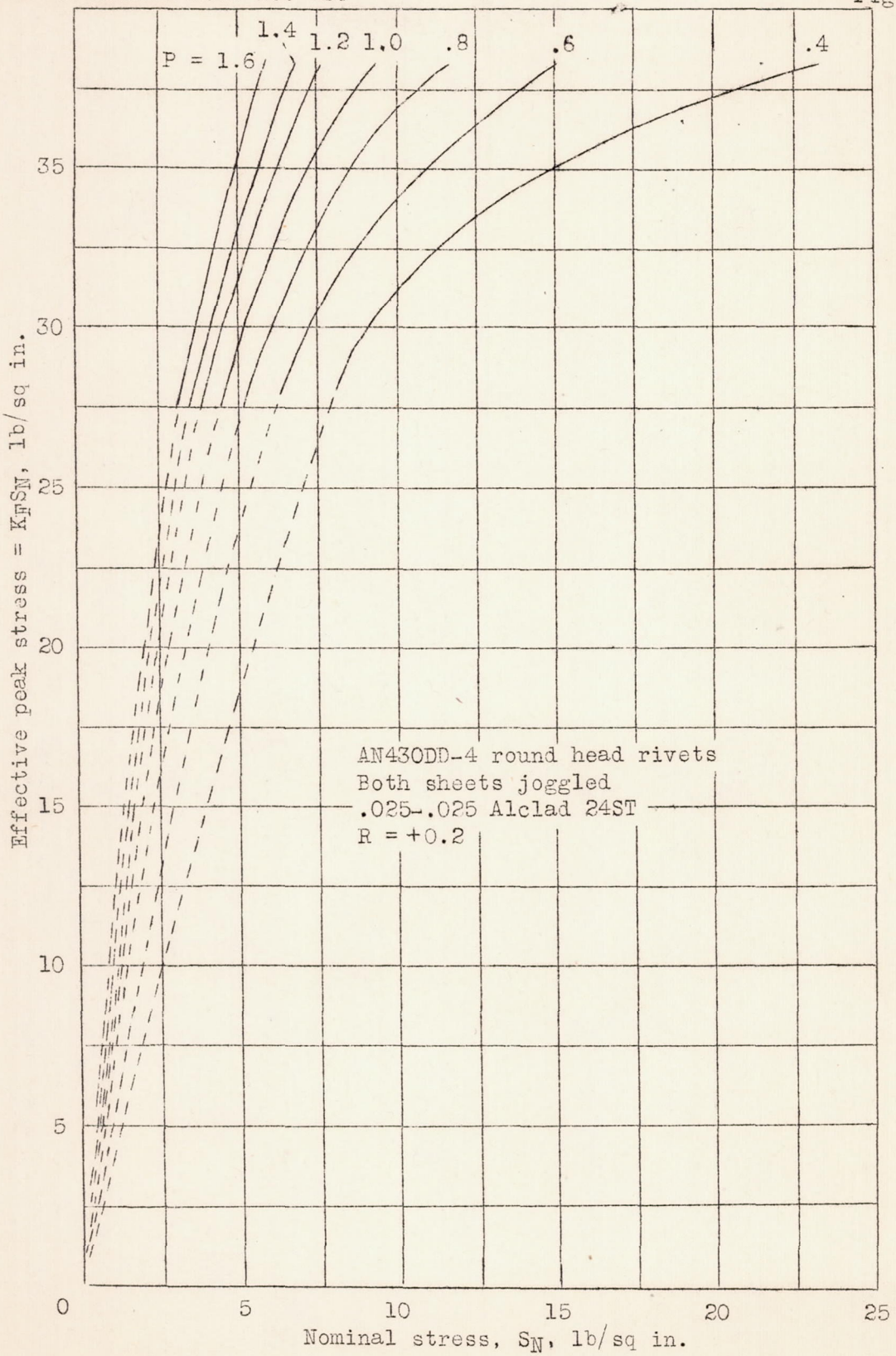

Figure 24.- Variation of effective peak stress with nominal stress for constant values of rivet pitch.

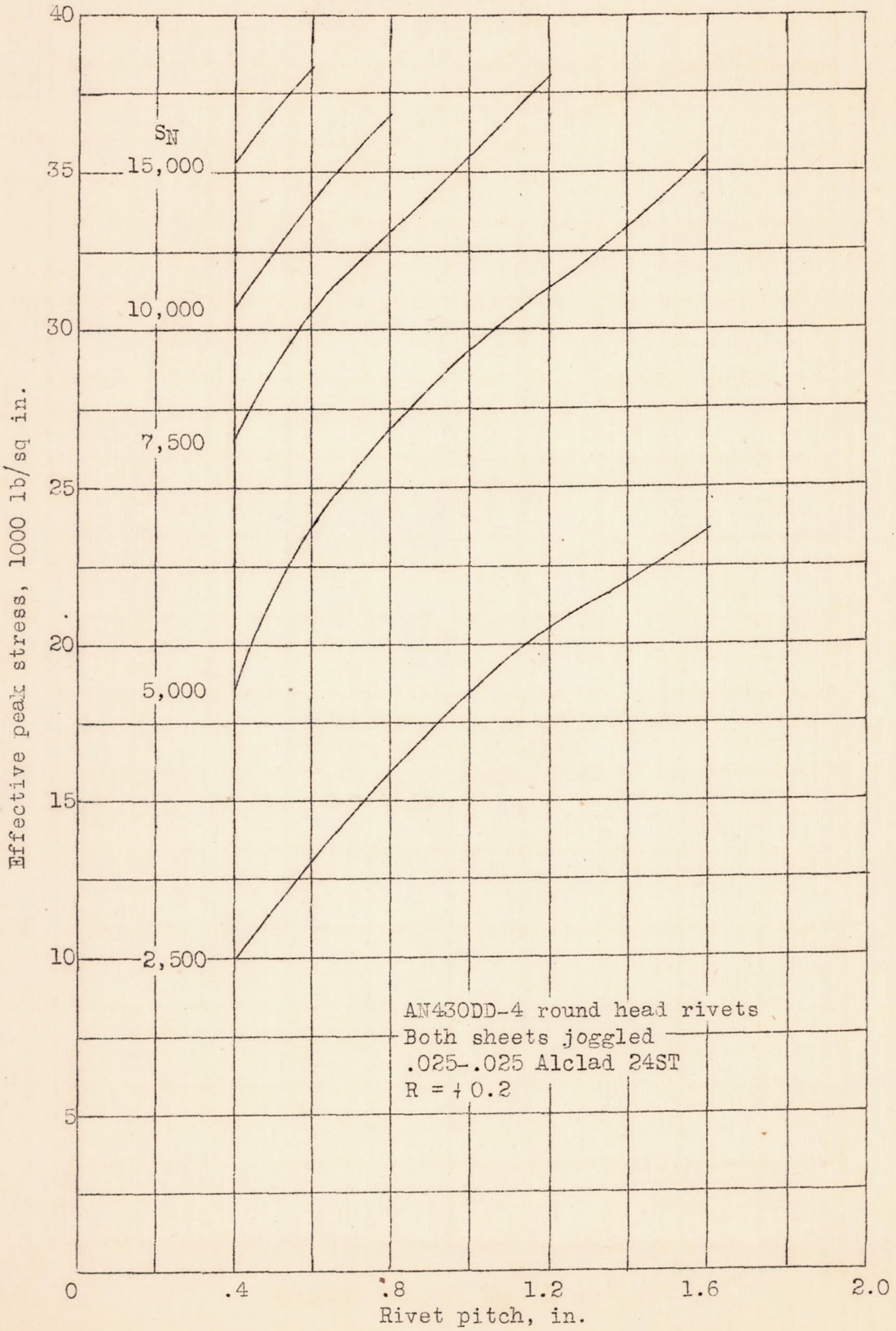

Figure 25.- Variation of effective peak stress with rivet pitch for constant values of nominal stress.

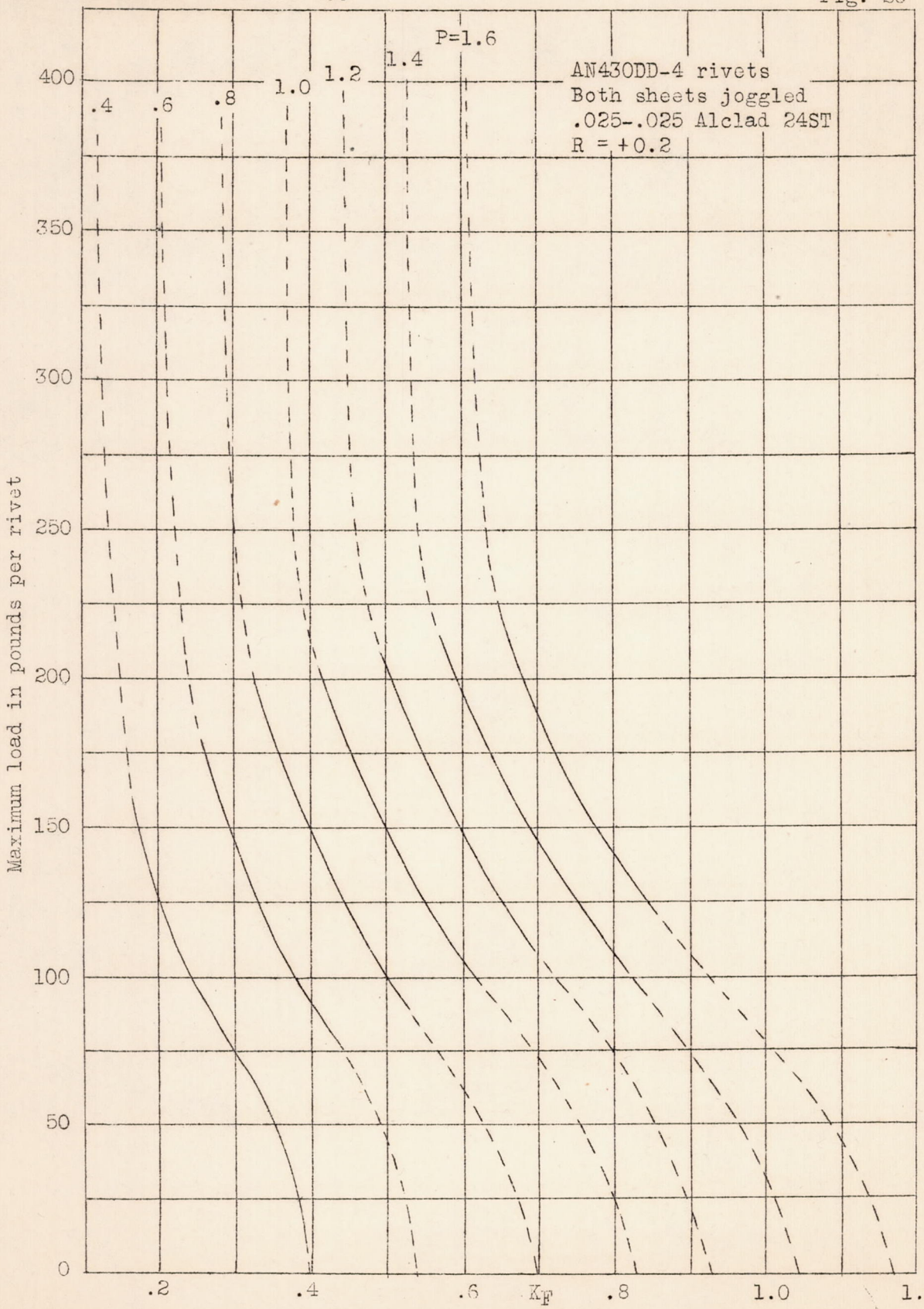

Figure 26.- Variation of the effective stress concentration factor in fatigue with maximum load per rivet for constant values of rivet pitch.

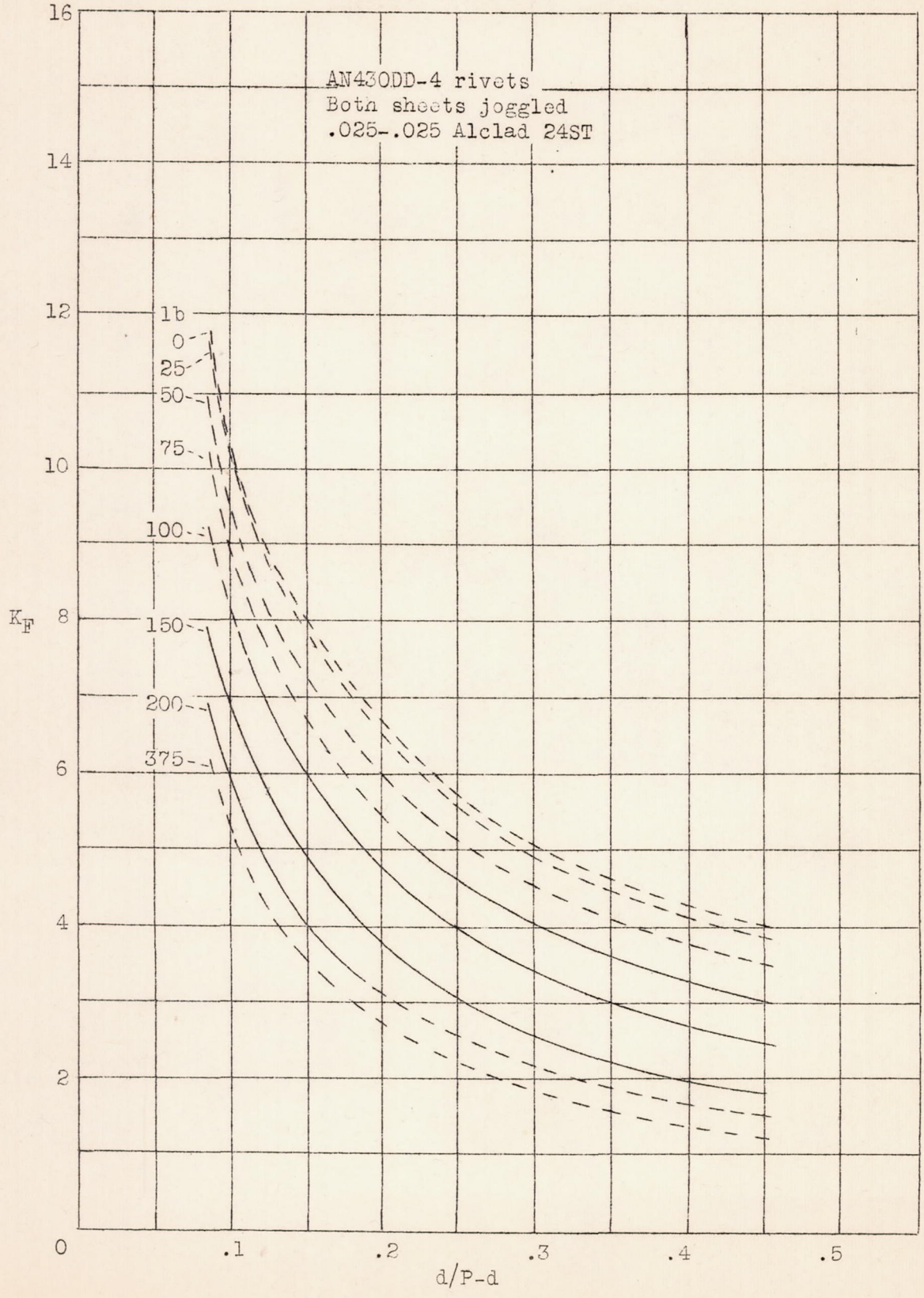

Figure 27.- Variation of K_F with net width of sheet supporting each rivet for constant values of load per rivet.

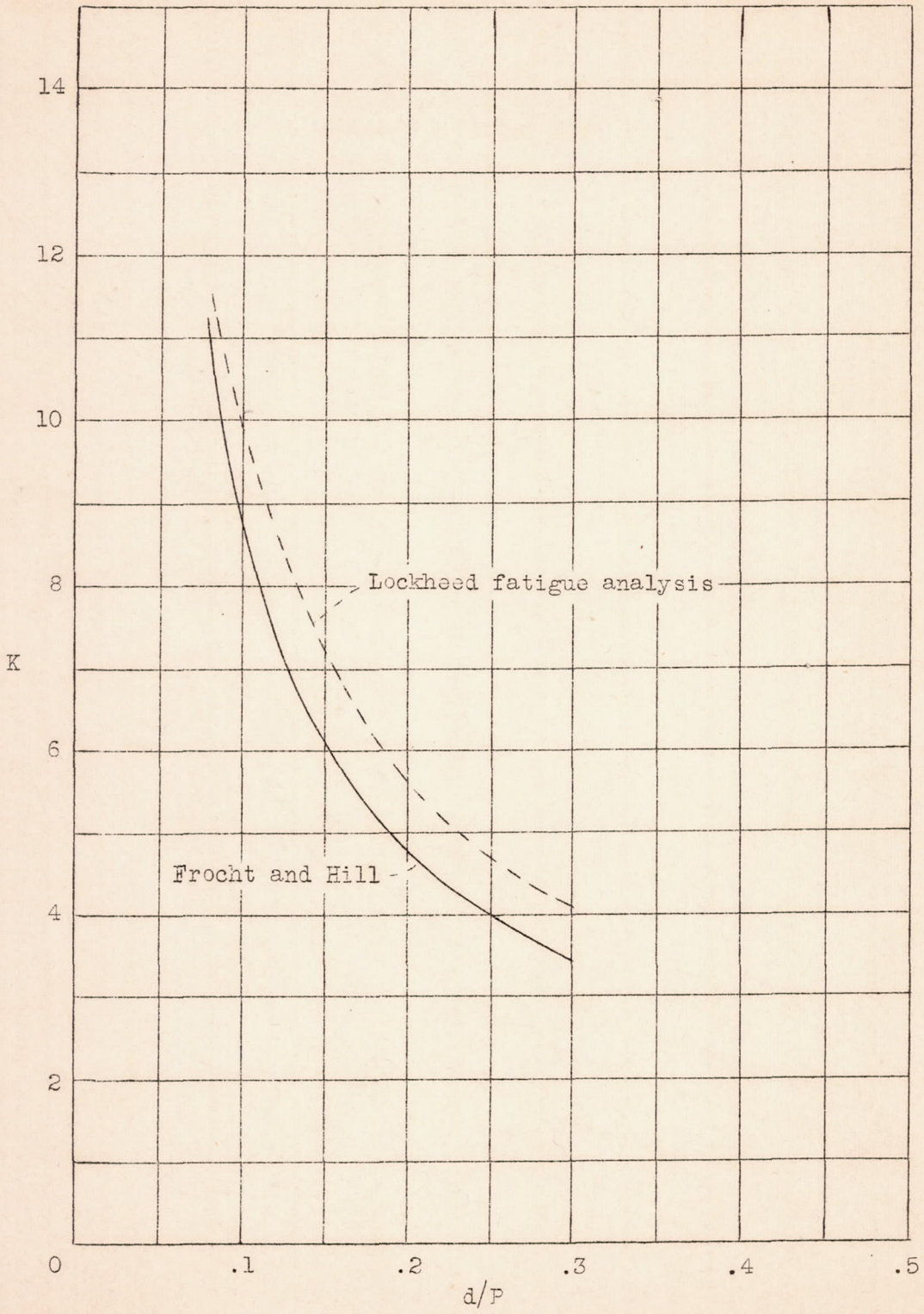

Figure 28.- K plotted against ratio of rivet diameter to rivet pitch for zero stress.